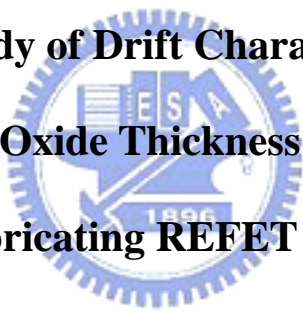# 國 立 交 通 大 學

電子工程學系 電子研究所碩士班

碩 士 論 文

臨場共製之 REFET 與 ISFET 對於感測氧化層厚度調變的
飄移特性之研究

The Study of Drift Characteristics

with Sense Oxide Thickness Modulation

by Co-Fabricating REFET and ISFET

學生: 徐信佑   Student: Hsin-Yu Hsu

指導教授: 張國明 博士   Advisor: Dr. Kow-Ming Chang

中華民國九十五年六月

臨場共製之 REFET 與 ISFET 對於感測氧化層厚度調變的

飄移特性之研究

The Study of Drift Characteristics

with Sense Oxide Thickness Modulation

by Co-Fabricating REFET and ISFET

研 究 生：徐信佑　　　　Student：Hsin-Yu Hsu

指導教授：張國明 博士　　Advisor：Kow-Ming Chang

國 立 交 通 大 學

電 子 工 程 學 系

碩 士 論 文

A Thesis

Submitted to Department of Electronics Engineering & Institute of Electronics

College of Electrical Engineering and Computer Science

National Chiao Tung University

in Partial Fulfillment of the Requirements

for the Degree of

Master of Science

in

Electronics Engineering

June 2006

Hsinchu, Taiwan, Republic of China

中華民國九十五年六月

臨場共製之 REFET 與 ISFET 對於感測氧化層厚度調變的飄移特性之研究

學生:徐信佑　　　　　　　　　　指導教授:張國明 博士

國立交通大學

電子工程學系　電子研究所碩士班

摘　　　要

　　本論文係利用電漿輔助化學氣象沈積的二氧化矽當作離子感測電晶體的感測材料，以及利用濺鍍的五氧化二鉭當作參照電晶體的感測材料，來研究其感測度及飄移特性。由此兩種材料製成的感測電晶體的感測度顯示，其感測特性主要是由材料的表面特性所影響。但是其飄移特性則是由材料的塊材特性所決定。飄移現象的產生是因為感測層材料表面的水合作用，以及氫離子在水合層中的殘留所造成。電漿輔助化學氣象沈積的二氧化矽材料會導致嚴重的水合作用，因此以此材料當作感測層的離子感測電晶體相對於其他材料的離子感測電晶體而言，會產生明顯的閘極電壓飄移現象。六小時的量測結果顯示，電漿輔助化學氣象沈積的二氧化矽材料層的水合深度大約是 500 埃，並且最大的閘極電壓飄移是 81 毫伏。
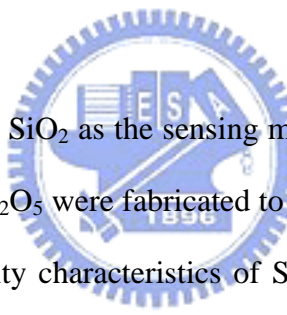
The Study of Drift Characteristics with Sense Oxide Thickness Modulation by Co-Fabricating REFET and ISFET

Student: Hsin-Yu Hsu   Advisor: Dr. Kow-Ming Chang

Department of Electronics Engineering & Institute of Electronics

National Chiao Tung University

ABSTRACT

The ISFETs of PECVD SiO_2 as the sensing membrane and the REFETs with a sensing layer of sputtered Ta_2O_5 were fabricated to study the sensitivity and the drift characteristics. The sensitivity characteristics of SiO_2-gate ISFETs and Ta_2O_5-gate REFETs showed that the pH responses were dependent on the surface characteristics of materials. But the drift characteristics were dependent on the characteristics of the material bulks. The drift phenomenon was due to the hydration effect of the sensing layer surface and the contamination of hydrogen ions in the hydrated layer. PECVD deposited SiO_2 can lead to a critical hydration effect such that the gate voltage drift of a PECVD SiO_2-gate ISFET is obvious relative to other ISFETs with sensing layers of different materials. In the measurement with duration of 6 hours, the hydration depth of a PECVD SiO_2 layer was about 500Å and the maximum gate voltage drift of a PECVD SiO_2-gate ISFET was 81mV.

誌　　謝

Contents

Table Captions

Figure Captions

Chapter 1

Introduction

1.1 The Importance of pH Detection

pH is one of the most common laboratory measurements because so many chemical and biomedical process are dependent on pH [1].

(1) Both the solubility of many chemicals or biomolecules in solution and the speed or rate of (bio-)chemical reactions are dependent on pH.

(2) The body fluid of living organisms usually has specific pH range that can reflect the health situation of the body. The pH values of lakes, rivers, oceans and soil differ and depend on the kinds of animals and plants living there. The wastewater from factories and households may cause the pH changes of water and cause the destruction of the environment.

(3) All the industries that deal with water: from the drinking water, the food and the drugs to the paper, plastics, semiconductors, cements, glass or textiles.

1.2 Techniques for pH Detection

Traditionally, the methods for the measurement of pH values include indicator reagents, pH test strips, metal electrode and glass electrode. Because of some limitations in practical applications of the first three methods, the glass electrode becomes the most widely used method for the pH measurement, and it is considered to be the standard measuring method.

The glass electrode is most widely used for pH measurement due to idea

Nernstian response independent of redox interferences, short balancing time of electrical potential, high reproducibility and long lifetime. However, glass electrode has several drawbacks for many industrial applications. Firstly, they are unstable in alkaline or HF solutions or at temperatures higher than $100°C$. Also, they exhibit a sluggish response and are difficult to miniaturize. Moreover, they cannot be used in food or in in vivo applications due to their brittle nature [1]. There is an increasing need for alternative pH electrodes.

New trends of pH measurements include optical-fiber-based pH sensor, mass-sensitive pH sensor, metal oxide sensor, conducting polymer pH sensor, nano-constructed cantilever-based pH sensor, ISFET-based pH sensor and pH-imaging sensor.

In this study, the problems in practical applications of ISFETs are continuing to be investigated.

1.3 The Problem of pH ISFET and the Investigation of this Problem

As mentioned in the first section, the environment of pH detection is always in a wet condition. That is, the devices used for the pH measurement must be immersed in the water solution, and then the sensing materials react with the solution and exhibit the pH responses. For ISFETs, the sensing materials used for pH detections are the gate oxides, such as SiO_2, Si_3N_4, Ta_2O_5, Al_2O_3, etc., however, these materials are not completely waterproof in nature. Some solution will permeate into the oxide surfaces and that may lead to the hydration effect. The hydration effect is a reaction correlated with time. The period of the hydration effect for Si_3N_4 to reach a steady state was about 50-60 hours in pH 7 solution [2], and for Al_2O_3 was about 7 hours [2].

Hydration effect is a critical problem in practical applications, and hence it limits

the commercialization speed and lowers the reliability of ISFET. Hydration can lead to a drift phenomenon of the gate voltage during the measurement, especially in the first two to three hours. When measuring the pH responses, the stability and accuracy are seriously influenced by the drift voltage.

In order to have a further understanding of the drift phenomenon, SiO_2 grown by plasma-enhanced chemical vapour deposition (PECVD) was used for the sensing layer of ISFET. PECVD SiO_2 is relatively poor in structural integrity and is expected to have an obvious hydration effect which can help us to observe the drift phenomenon more clearly. Detailed experiment steps will be presented in chapter 3, and the results will be discussed in chapter 4.

Chapter 2

Theories for the Investigation of Drift Characteristics

2.0 Introduction

In this chapter, the theories of metal oxide semiconductor field effect transistor (MOSFET) which are relevant to ISFET will firstly be presented. The fundamental principles of ISFET will be developed from these MOSFET theories. The pH response at the oxide-electrolyte interface will also be characterized in the first section. Subsequently, the drift phenomenon which is caused by the hydration effect and the ions transport in the insulator will be discussed. In the final section, a physical model for drift developed by Jamasb [12] will be presented. This model can help us to have a further understanding of the mechanism responsible for the instability of ISFET under long-term operating.
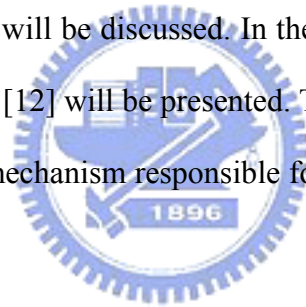
2.1 Fundamental Principles of ISFET

Since the first report of the ISFET by Bergveld, research on new material and fabrication process to improve the sensitivity and stability has been continuously proposed [3-5]. At the same time, the mechanism of the pH response of pH ISFET has also been studied extensively [4-10]. The followings are the theoretical foundations which are mostly adopted to characterize the ISFET.

2.1.1 From MOSFET to ISFET

Seen by the history of the development of ISFET, it is not difficult to find out the similarities between ISFET and MOSFET. The most obvious characteristic is the similarity between their structures. Therefore, the best way to comprehend the ISFET is to understand the operating principle of a MOSFET first. When MOSFET is operated in the so-called ohmic or non-saturated region, the drain current I_D is given by:

$$I_D = \frac{C_{OX}\mu W}{L}\left\{(V_{GS} - V_T) - \frac{1}{2}V_{DS}\right\}V_{DS}$$ (2-1)

where C_{OX} is the gate insulator capacitance per unit area, μ the electron mobility in the channel and W/L the width-to-length ratio of the channel.

The threshold voltage V_T of Eq. (2-1) is described by the following expression:

$$V_T = V_{FB} - \frac{Q_B}{C_{OX}} + 2\phi_F$$ (2-2)

where V_{FB} is the flat-band voltage, Q_B the depletion charge in the substrate, and ϕ_F the potential difference between the Fermi levels of doped and intrinsic silicon. For a MOSFET with charge present in the oxide and at the oxide-semiconductor interface, the flat-band voltage can be given by:

$$V_{FB} = \frac{\Phi_M - \Phi_{Si}}{q} - \frac{Q_{OX} + Q_{SS}}{C_{OX}}$$ (2-3)

where Φ_M is the workfunction of the gate metal, Φ_{Si} the workfunction of silicon, Q_{OX} the charge in the oxide and Q_{SS} the surface state density at the oxide-silicon interface. Substitution of Eq. (2-3) in Eq. (2-2), the general form of the threshold voltage of a MOSFET becomes:

$$V_T = \frac{\Phi_M - \Phi_{Si}}{q} - \frac{Q_{OX} + Q_{SS} + Q_B}{C_{OX}} + 2\varphi_F$$ (2-4)

This equation holds true for the metal gate MOSFET. But in case of the ISFET, the metal gate is no longer present, so that the term Φ_M/q must be revised. Figure 2-1 illustrates the similarities and differences between these two devices. It can be seen

that the reference electrode, the aqueous solution and the phenomena occurring at the oxide-solution interface must be accounted for instead of Φ_M/q. Hence the threshold voltage of the ISFET becomes:

$$V_T = E_{ref} + \chi^{sol} - \Psi_0 - \frac{\Phi_{Si}}{q} - \frac{Q_{OX} + Q_{SS} + Q_B}{C_{OX}} + 2\varphi_F \qquad (2\text{-}5)$$

where E_{ref} represents the constant potential of the reference electrode, χ^{sol} is the surface dipole potential of the solution which also has a constant value. The term Ψ_0 representing the surface potential at the oxide-electrolyte interface is the key element that makes ISFET pH-sensitive.

2.1.2 The pH Response at Oxide-Electrolyte Interface

The surface of any metal oxide always contains hydroxyl groups, in the case of silicon dioxide SiOH groups. These groups can be protonated and deprotonated, and thus, when the gate oxide contacts an aqueous solution, a change of pH will change the SiO_2 surface potential. These reactions can be expressed by

$$H_S^+ + SiOH \xleftrightarrow{\;K_1\;} SiOH_2^+ \qquad (2\text{-}6)$$

$$SiOH \xleftrightarrow{\;K_2\;} SiO^- + H_S^+ \qquad (2\text{-}7)$$

where H_S^+ represents the protons at the surface of the oxide.

The pH response, which is generally called the sensitivity, is defined as the surface potential change over a pH unit change. This response is given by

$$\frac{\delta \Psi_0}{\delta pH_B} = -2.3 \frac{kT}{q} \alpha \qquad (2\text{-}8)$$

with

$$\alpha = \frac{1}{\dfrac{2.3 kT C_{dif}}{q^2 \beta_{int}} + 1} \qquad (2\text{-}9)$$

where pH_B is the pH value in the solution bulk, k is the Boltzmann constant, T is the absolute temperature, C_{dif} is the differential capacitance, and β_{int} is the intrinsic buffer capacity. α is a dimensionless sensitivity parameter. The value of α varies between 0 and 1 depending on the intrinsic buffer capacity and the differential capacitance. If α equals 1, the theoretical maximum sensitivity of -59.2mV/pH at room temperature can be obtained.

The potential between electrolyte solution and insulator surface causes a proton concentration difference between bulk and surface that is according to Boltzmann:

$$a_{H_S^+} = a_{H_B^+} \exp \frac{-q\Psi_0}{kT} \tag{2-10}$$

where $a_{H_S^+}$ and $a_{H_B^+}$ are the activity of H$^+$ at the oxide surface and in the solution bulk, respectively. According to the definition of pH, Eq. (2-10) can be expressed by

$$pH_S = pH_B + \frac{q\Psi_0}{2.3kT} \tag{2-11}$$

(2-11) correlates the pH$_S$ in (2-6) and (2-7) with the pH$_B$ in (2-8).
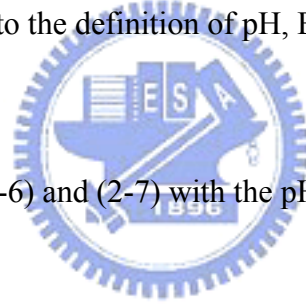
2.2 Drift Phenomenon

Drift phenomenon can be considered by two aspects of view, the hydration of the insulator surface after immersing it in pH buffer solution, and the trap of hydrogen-bearing species by the binding sites when they transport through the insulator. The former's influence on drift is generally smaller than the latter. This result can be found in the previous work [2, 11-13] and also in the measurement data of this research. The following models, which are classified according to the location where the mechanism of pH-sensitivity is presumed to occur, will help us to have a further understanding of the transport of mobile ions [14]:

(1) Models based on the reactivity of the insulator surface. The surface sites on

the insulator react with ions in the solution and build up a surface potential. This will lead to the formation of the electrical double layer in the electrolyte at the interface with the insulator. This model is generally regarded as the site-binding model.

(2) Models based on the presence of mobile ions in the insulating layer. This implies the existence of a transport mechanism to establish the required thermodynamic equilibrium, and leads directly to a Nernst equation. This model is generally regarded as the gel model.

(3) Models based on the modification of the Si/SiO_2 interface through a pH-controlled change in the surface state density via transport of a hydrogen-bearing species.

The above discussions are only the characteristics of ions transport in the insulator, while the physical model for the gate voltage drift is going to be presented in the next section.
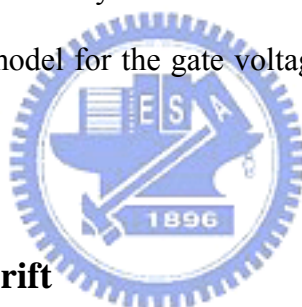
2.3 Physical Model for Drift

The physical model for drift was firstly proposed by Jamasb in 1997 [11]. The key point of this model was that employing the dispersive transport theory to express the gate voltage drift which is caused by the hydration effect at the insulator-electrolyte interface.

2.3.1 Dispersive Transport

Dispersive transport was brief reviewed in [12] and it could be characterized by a power-law time decay of the mobility or diffusivity of the form $t^{\beta-1}$, $0<\beta<1$. This time dependence is based on a model that interprets transport in terms of a "random walk".

The origin of random walk is either a) hopping motion through localized states giving rise to hopping transport, or b) multiple trapping from a band of extended states or localized states leading to multiple-trap transport. The multiple-trap transport is generally associated with the motion of electrons or holes in disordered materials.

Regardless of the specific dispersive mechanism involved, dispersive transport leads to a characteristic power-law time decay of diffusivity which can be described by

$$D(t) = D_{00}(\omega_0 t)^{\beta-1} \tag{2-12}$$

where D_{00} is a temperature-dependent diffusion coefficient which obeys an Arrhenius relationship, ω_0 is the hopping attempt frequency, and β is the dispersion parameter satisfying $0<\beta<1$. Dispersive transport leads to a decay in the density of sites/traps occupied by the species undergoing transport. This decay is described by the stretched-exponential time dependence given by

$$\Delta N_{S/T}(t) = \Delta N_{S/T}(0)\exp[(-t/\tau)^{\beta}] \tag{2-13}$$

where $\Delta N_{S/T}(t)$ is the area density (units of cm^{-2}) of sites/traps occupied, τ is the time constant associated with structural relaxation, and β is the dispersion parameter.

2.3.2 Expression for Drift

Since hydration leads to a change of the chemical composition of the sensing oxide surface, it is reasonable to assume that the dielectric constant of the hydrated surface layer differs from that of the sensing oxide bulk. The overall insulator capacitance, which is determined by the series combination of the surface hydration layer and the underlying oxide, will exhibit a slow, temporal change. When drift phenomenon occurs at the surface of an actively-biased ISFET, the gate voltage will

simultaneously exhibit a change to keep a constant drain current. The change of the gate voltage can be written as

$$\Delta V_G(t) = V_G(t) - V_G(0) \tag{2-14}$$

Since the voltage drop inside of the semiconductor is kept constant, $\Delta V_G(t)$ becomes

$$\Delta V_G(t) = [V_{FB}(t) - V_{FB}(0)] + [V_{ins}(t) - V_{ins}(0)] \tag{2-15}$$

where V_{FB} is the flatband voltage and V_{ins} is the voltage drop across the insulator. V_{FB} and V_{ins} are given by

$$V_{FB} = E_{ref} + \chi^{sol} - \Psi_0 - \frac{\Phi_{Si}}{q} - \frac{Q_{OX} + Q_{SS}}{C_{OX}} \tag{2-16}$$

$$V_{ins} = \frac{-(Q_B + Q_{inv})}{C_{OX}} \tag{2-17}$$

where Q_{inv} is the inversion charge. If the temperature, pH, and the ionic strength of the solution are held constant, $E_{ref,}\chi^{sol}$, Ψ_0, and Φ_{Si} can be neglected, so the drift can be rewritten as

$$\Delta V_G(t) = -(Q_{OX} + Q_{SS} + Q_B + Q_{inv}) \left[\frac{1}{C_i(t)} - \frac{1}{C_I(0)} \right] \tag{2-18}$$

In this study, the gate oxide of the fabricated ISFET was composed of two layers, a lower layer of thermally-grown SiO_2 of thickness, x_L, and an upper layer of PECVD SiO_2 of thickness, x_U. $C_I(0)$ is the effective insulator capacitance given by the series combination of the thermally-grown SiO_2 capacitance, ε_L/x_L, and the PECVD SiO_2 capacitance, ε_U/x_U. $C_i(t)$ is analogous to $C_I(0)$, but an additional hydrated layer of capacitance, ε_{HL}/x_{HL}, at the oxide-electrolyte interface must be took into consideration, and the PECVD SiO_2 capacitance is now given by $\varepsilon_U/[x_U - x_{HL}]$. The series combinations of the capacitances are illustrated in Figure 2-2. Therefore, the drift is given by

$$\Delta V_G(t) = -(Q_{OX} + Q_{SS} + Q_B + Q_{inv}) \left(\frac{\varepsilon_U - \varepsilon_{HL}}{\varepsilon_U \varepsilon_{HL}} \right) x_{HL}(t) \tag{2-19}$$

From this equation, we observed that drift is directly proportional to the thickness of the hydrated layer. By applying dispersive transport theory, an expression for $x_{HL}(t)$ is given by [12]

$$x_{HL}(t) = x_{HL}(\infty)\left\{1 - \exp\left[-(t/\tau)^{\beta}\right]\right\} \tag{2-20}$$

with

$$x_{HL}(\infty) = \frac{D_{00}\omega_0^{\beta-1}\Delta N_{S/T}(0)}{A_D \beta N_{hydr}} \tag{2-21}$$

where A_D represents the cross-sectional area, and N_{hydr} is the average density of the hydrating species per unit volume of hydration layer. Thus, the overall expression for the gate voltage drift is

$$\Delta V_G(t) = -(Q_{OX} + Q_{SS} + Q_B + Q_{inv})\left(\frac{\varepsilon_U - \varepsilon_{HL}}{\varepsilon_U \varepsilon_{HL}}\right)x_{HL}(\infty)\left\{1 - \exp\left[-(t/\tau)^{\beta}\right]\right\} \tag{2-22}$$

From this equation, we can expect that if the time of gate oxide immersing in the test-solution is long enough (determined by the constant τ), the gate voltage drift will approach a constant value which is greatly dependent on the hydration depth, $x_{HL}(\infty)$.

Chapter 3

Experiment and Measurement

3.0 Introduction

In this chapter, the advantage of making differential measurements between an ISFET and a reference FET (REFET) will be interpreted in the first section. The importance of a stable reference electrode (RE) in the miniaturized device will also be discussed. The second section is the fabrication process flow of the ISFET and REFET devices which are used for investigating the drift characteristics. Finally, the measurement setup, and the detection principles of pH and drift will be presented.

3.1 Differential Sensing

How to detect a correct and consistent pH value is always the direction of research. Besides adopting materials that have good linearity, sensitivity, and stability, there are two important subjects in measurement that provide alternative ways to obtain a reliable pH value. One is the design of a stable reference electrode, the other is the introduction of a REFET.

3.1.1 Reference Electrode

An ideal reference electrode for use as the ISFET gate terminal should provide [15]

a) an electrical contact to the solution from which to define the solution potential;

b) an electrode/solution potential difference (E_{ref}) that does not vary with solution composition.

The conventional silver chloride or calomel electrode provides both of these functions by maintaining an electrochemical equilibrium with the solution. Novel techniques are to fabricate the reference electrodes in miniaturized dimensions [16,17]. The on-chip fabrication of a reference electrode with IC-compatible techniques would make ISFETs suitable for biomedical sensing because of the low cost, small size and rigidity.

3.1.2 Reference FET

An alternative technique to achieve consistent pH detections is through the co-fabricating of an ISFET and a REFET. An ideal REFET is a FET that insensitive to ions in pH measurement [18], but identical to the ISFET in terms of transconductance, thermal response, etc. The differential measurement between an ISFET and a REFET thus eliminates the variations of the environment, such as temperature, light, instable reference electrode/solution contact potential, etc.

In this study, an alternative approach to the implementation of a REFET is introduced. Ta_2O_5 is a material that exhibits good linearity, sensitivity, and stability in the pH measurement, so we are trying to take this material as the sensing layer material instead of an ion-insensitive one.

3.2 Fabrication Process

As mentioned in the previous section, Ta_2O_5 was taken as the sensing layer material of REFET, while SiO_2 was the sensing material of ISFET. Ta_2O_5 was

deposited by sputtering, and SiO$_2$ was deposited using plasma-enhanced chemical vapour deposition (PECVD). Because of the relatively low deposition temperature, PECVD SiO$_2$ is poor in structural integrity in comparison with other preparation methods, such as LPCVD and thermally grown silica [19]. The poor integrity of the gate oxide structure is expected to have an obvious hydration effect which can help us to observe the drift phenomenon more clearly during the pH measurement. The following is the procedure for fabricating the ISFET and REFET devices, and the process is illustrated in Figure 3-1:

a) RCA clean

　　Wet-oxidation, 6000Å, 1050°C

b) Defining of S/D (mask 1)

　　BOE wet-etching of SiO$_2$

c) Dry-oxidation, 300Å, 1050°C

　　S/D ion implantation

　　S/D annealing, 950°C, 60min
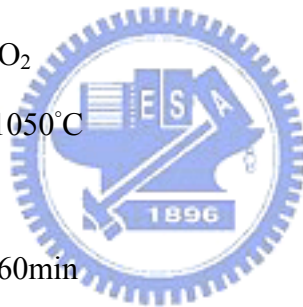
d) PECVD SiO$_2$ for passivation, 1μm

e) Defining of contact hole and gate region (mask 2)

　　BOE wet-etching of SiO$_2$

f) Dry growth of gate oxide, 100Å, 850°C

g) PECVD SiO$_2$ as sensing layer, 4 conditions are prepared, 100Å, 300Å, 500Å, 1000Å

　　Defining of sensing region (mask 3)

　　HF wet-etching of SiO$_2$

h) Sputtering Ta$_2$O$_5$ as sensing layer, 300Å (mask 4)

　　Ta$_2$O$_5$ sintering, 600°C, 30min

i) Al evaporation, 5000Å (mask 5)

Al sintering, 400°C, 30min

3.3 Measurement Principle

The setup of the measurement system is illustrated in Figure 3-2. ISFET and REFET were designed to share the same source terminal, and the drain-to-source voltage were biased at the same condition ($V_{DS1}=V_{DS2}$). The drain currents of ISFET and REFET were set at a constant magnitude, therefore, if the pH of the solution varies, the gate voltage must adjust its magnitude to maintain the constant current. Consequently, the variation of the gate voltage exhibits the pH sensitivity of the sensing oxide. Figure 3-3 illustrates the detection principle of pH. For the drift measurement, the detection principle is in a similar manner to that of the pH measurement and is shown in Figure 3-4.
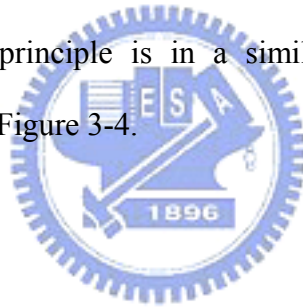
Chapter 4

Results and Discussions

4.1 Sensitivities of PECVD SiO$_2$ and Sputtered Ta$_2$O$_5$

Figure 4-1~4-12 are the measured sensitivities of PECVD SiO$_2$ and sputtered Ta$_2$O$_5$, and the data are sorted in Table 4-1. The samples of SiO$_2$ were prepared in dimensions of W/L=400μm/20μm, 400μm/30μm and 400μm/40μm as well as in thickness of 100Å, 300Å, 500Å and 1000Å. But the Ta$_2$O$_5$-gate REFETs were of the thickness of 300Å only. Followings are the discussions of the measurement results:

(1) *The variations in thickness of the SiO$_2$ sensing oxide showed no influence on the sensitivity*. This result can be explained by the Nernst equation for sensitivity and also the site-dissociation model [10] that the pH sensitivity is presumed to occur at the surface of the sensing layer.

(2) *There is no consistency of sensitivities among the PECVD SiO$_2$-gate ISFETs*. For PECVD deposited SiO$_2$ films, lacking of uniformity were innate problems such that the PECVD SiO$_2$-gate ISFET devices, even were fabricated on the same wafer, could exhibit different characteristics.

(3) *Devices of different dimensions have no critical influence on the sensitivity*. As what have been discussed in (2) and (3), the sensitivity of ISFET device was determined by the surface characteristics of its specific sensing film, but not by the FET device itself.

(4) *Ta$_2$O$_5$ shows a good linearity of the sensitivity from pH 1 to pH 13, and it also has a high sensitivity of 54.6mV/pH in average*.

(5) *The sensitivity of SiO$_2$ is relatively higher in the pH range of 1-9 than in*

the range of 9-13.

(6) *By Taking Ta$_2$O$_5$-ISFET as the REFET, the SiO$_2$-ISFET exhibits a relatively higher sensitivity in the pH range of 9-13*. It is contrary to the result of applying solely a SiO$_2$-ISFET that the sensitivity is relatively lower in the pH range of 9-13.

4.2 Drift Characteristics

Drift characteristics of PECVD SiO$_2$-gate ISFETs are shown in Figure 4-13~4-16. Measurements were carried out in pH 7, and the duration of each measurement was about 6 hours. Average drift rate per hour was calculated by averaging the gate voltage drift in the last 5 hour, the results were 7.4, 12.8, 15.4 and 16.2mV/hour for 100Å, 300Å, 500Å and 1000Å of PECVD SiO$_2$ respectively. These results are listed in table 4-2. Figure 4-18 shows the drift characteristic of Ta$_2$O$_5$. The measured drift rate of Ta$_2$O$_5$ was 1.6mV/hour. Followings are the discussions of the drift characteristics:

(1) *The drift rate of 300Å SiO$_2$ has a critical increase from 100Å SiO$_2$*. This critical increase reflects that the 300Å SiO$_2$ captures more H$^+$ ions than 100Å SiO$_2$ can do in the same time duration. However, the transport of H$^+$ ions is presumed that it takes place in the hydrated layer because the hydration layer has a sufficiently open structure that ionic mobilities are much higher than in the rigid bulk region [14]. That is, 300Å SiO$_2$ has a deeper hydration depth and more binding sites than 100Å SiO$_2$. This suggests that the 100Å SiO$_2$ is fully hydrated, and the 100Å hydration depth of a PECVD-deposited SiO$_2$ film is reasonable in comparison with the LPCVD-grown Si$_3$N$_4$ film that has a hydration depth of about 105Å [12].

(2) *The drift rate of 500Å SiO$_2$ also has a critical increase from 300Å SiO$_2$, but*

the increment is not as large as that from 100Å to 300Å. The explanation is same as it of (1), and the 300Å SiO$_2$ is suggested fully hydrated. The large hydration depth of the SiO$_2$ film is reasonable to a PECVD-related process that has a lattice structure not as dense as a high-temperature process.

(3) ***The drift rate of 1000Å SiO$_2$ has only increased by 5% from 500Å SiO$_2$***. It suggests that 500Å SiO$_2$ has almost provided an enough thickness for the maximum hydration depth it may reach after 6 hours of hydrating as well as 1000Å SiO$_2$ can do.

(4) ***The drift rate of PECVD SiO$_2$ is obviously larger then other sensing oxides proposed in the literature*** [20] ***such as Al$_2$O$_3$ and Si$_3$N$_4$, and it is also larger than the measured drift rate of Ta$_2$O$_5$ of this research***. This result is consistent with the expectation of the drift rate of PECVD SiO$_2$ mentioned in chapter 3.

(5) ***The initial drift rates of the four samples are roughly the same in the initially first hour, and the drift of the gate voltage is obviously larger than the total amount in the last 5 hours***. It was regarded that the density of Si-OH sites near the SiO$_2$ surface was large, and the OH sites buried in SiO$_2$ was several orders in density smaller than the surface OH sites [14].

From (1), (2) and (3) it is not hard to figure out that the hydration depth is around 500Å, therefore, a thickness of larger than 500Å will not efficiently provide additional space for exchanging of H$^+$ ions. The average drift rate is illustrated in Figure 4-17.

4.3 Conclusions

The ISFETs of PECVD SiO$_2$ as the sensing membrane and the REFETs with a sensing layer of sputtered Ta$_2$O$_5$ were fabricated. The sensitivities of SiO$_2$-gate ISFETs showed no consistency among the devices while the Ta$_2$O$_5$-gate REFETs were good in stability and linearity of the sensitivity characteristics. The sensitivities of

PECVD SiO_2-gate ISFETs was relatively low in pH 9-13, but was relatively high in the same pH range through differential sensing with Ta_2O_5-gate REFETs. The drift characteristics of the four thickness conditions of PECVD SiO_2 suggested that the hydration depth, or the space for exchanging of H^+ ions, was around 500Å. This depth was obviously larger than other materials prepared by other methods, e.g. sputtered Ta_2O_5, LPCVD Si_3N_4, thermal SiO_2, sputtered Al_2O_3, etc. The drift rate in the first hour was large because of the large density of Si-OH sites near the SiO_2 surface, while the density of buried OH sites below the surface was relatively small to the surface.

Chapter 5

Future Work

5.1 Electric Field Enhanced Migration of Hydrogen Ions

The H^+ ions may be influenced by the electric field applied by the gate electrode when migrating in the insulator. Therefore, the observation of the migration behavior of H^+ ions under different electric field strength conditions is a critical subject. Figure 5-1 is the illustration of the H^+ ions contamination influenced by different electric field strength.

References

[1] Y. Q. Miao, J. R. Chen and K. M. Fang, New technology for the detection of pH, J. Biochem. Biophys. Methods **63** (2005) 1-9.

[2] S. Jamasb, S. Collins and R.L. Smith, A physical model for drift in pH ISFETs, Sens. Actuators B **49** (1998) 146-155.

[3] Tadayuki Matsuo and Masayoshi Esashi, Methods of ISFET fabrication, Sens. Actuators **1** (1981) 77-96.

[4] Massimo Grattarola and Giuseppe Massobrio, Bioelectronics handbook: MOSFETs, biosensors, and neurons, McGraw-Hill, New York, 1998.

[5] P. Bergveld, Thirty years of ISFETOLOGY: What happened in the past 30 years and what may happen in the next 30 years, Sens. Actuators B **88** (2003) 1-20.

[6] Wouter Olthuis, Chemical and physical FET-based sensors or variations on an equation, Sens. Actuators B **105** (2005) 96-103.

[7] D.E. Yates, S. Levine and T.W. Healy, Site-binding model of the electrical double layer at the oxide/water interface, J. Chem. Soc., Faraday Trans. **70** (1974) 1807-1818.

[8] Luc Bousse, Nico F. de Rooij and P. Bergveld, Operation of chemically sensitive field-effect sensors as a function of the insulator-electrolyte interface, IEEE Trans. Electron Devices **ED-30** (1983) 1263-1270.

[9] R.E.G. van Hal, J.C.T. Eijkel and P. Bergveld, A novel description of ISFET sensitivity with the buffer capacity and double-layer capacitance as key parameters, Sens. Actuators B **24-25** (1995) 201-205.

[10] R.E.G. van Hal, J.C.T. Eijkel and P. Bergveld, A general model to describe the electrostatic potential at electrolyte oxide interfaces, Adv. Coll. Interf. Sci. **69** (1996)

31-62.

[11] S. Jamasb, S. Collins and R.L. Smith, A physically-based model for drift in Al$_2$O$_3$-gate pH ISFET's, Tech. Digest, 9th Int. Conf. Solid-State Sensors and Actuators (Transducers '97), Chicago, IL, 15-19 June, 1997, 1379-1382.

[12] S. Jamasb, S.D. Collins and R.L. Smith, A physical model for threshold voltage instability in Si$_3$N$_4$-gate H^{+}-sensitive FET's (pH ISFET's), IEEE Trans. Electron Devices **45** (1998) 1239-1245.

[13] S. Jamasb, An analytical technique for counteracting drift in Ion-Selective Field Effect Transistors (ISFETs), IEEE Sens. J. **4** (2004) 795-801.

[14] Luc Bousse and P. Bergveld, The role of buried OH sites in the response mechanism of inorganic-gate pH-sensitive ISFETs, Sens. Actuators **6** (1984) 67-78.

[15] P.A. Hammond, D. Ali and D.R.S. Cumming, Design of a single-chip pH sensor using a conventional 0.6-μm CMOS process, IEEE Sens. J. **4** (2004) 706-712.

[16] R.L. Smith and D.C. Scott, An integrated sensor for electrochemical measurements, IEEE Trans. Biomed. Eng. BME **33** (1986) 83-90.

[17] I.Y. Huang and R.S. Huang, Fabrication and characterization of a new planar solid-state reference electrode for ISFET sensors, Thin Solid Films **406** (2002) 225-261.

[18] A. Errachid, J. Bausells and N. Jaffrezic-Renault, A simple REFET for pH detection in differential mode, Sens. Actuators B **60** (1999) 43-48.

[19] A.R. Barron, CVD of SiO$_2$ and related materials: an overview, Adv. Mater. Opt. Elec. **6** (1996) 101-114.

[20] J.L. Chiang, J.C. Chou, Y.C. Chen, G.S. Liau and C.C. Cheng, Drift and hysteresis effect on AIN/SiO$_2$ Gate pH ion-sensitive field-effect transistor, Jpn. J. Appl. Phys. **42** (2003) 4973-4977.

電解質 (electrolyte) diagram
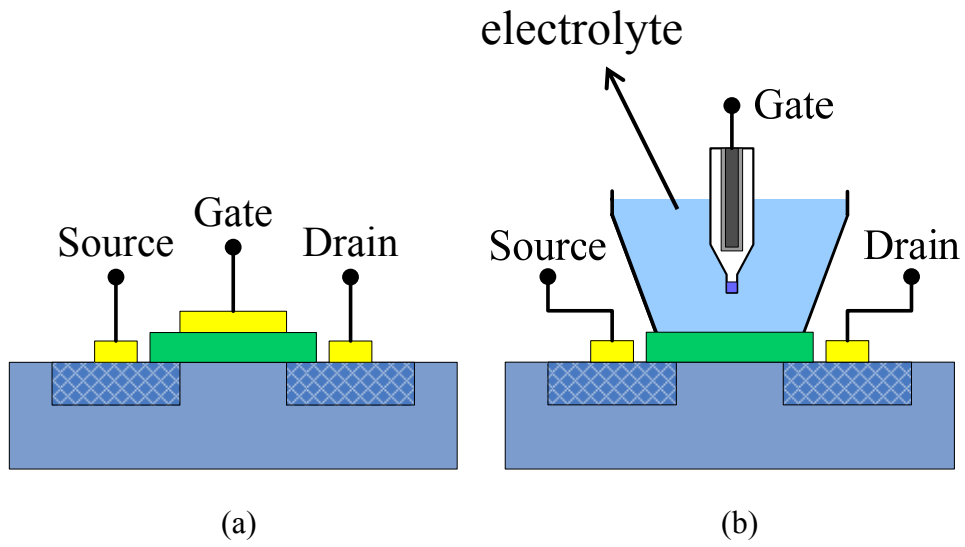
Fig. 2-1 Schematic representation of (a) MOSFET, (b) ISFET
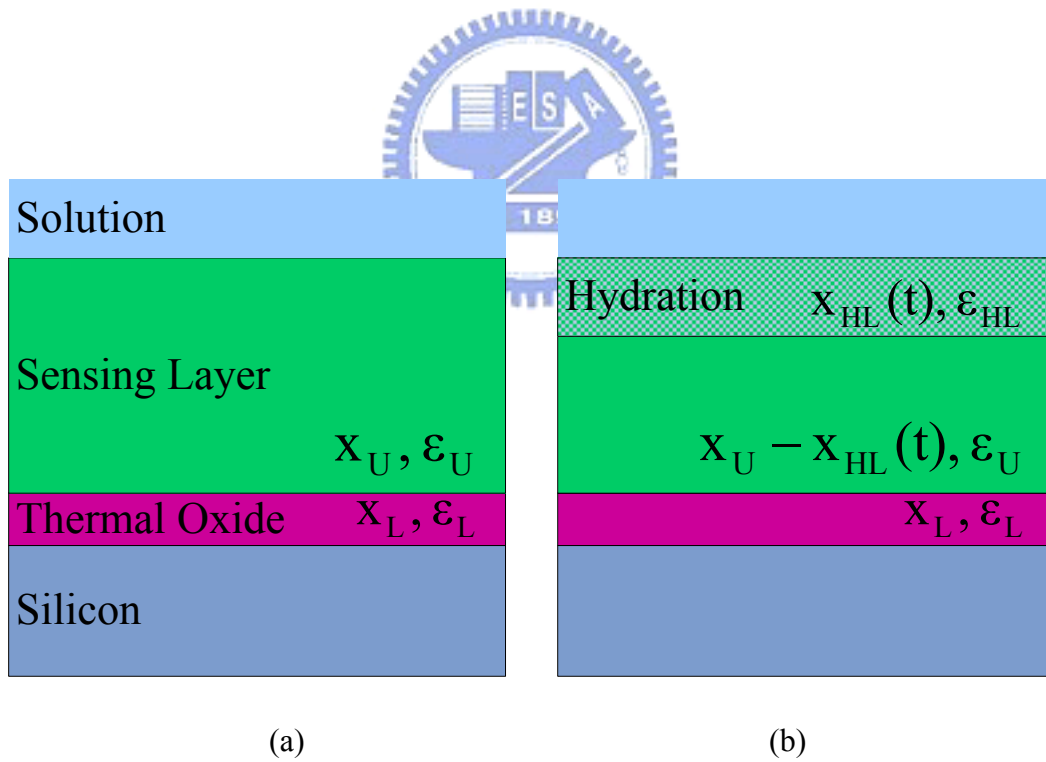
Fig. 2-2 Series combination of the (a) initial (b) hydrated insulator capacitance

(a)
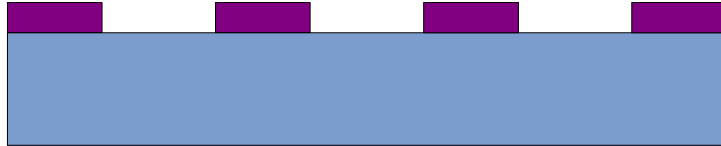
(b)
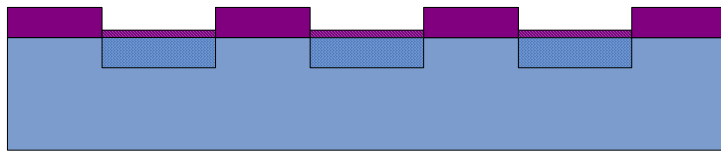
(c)
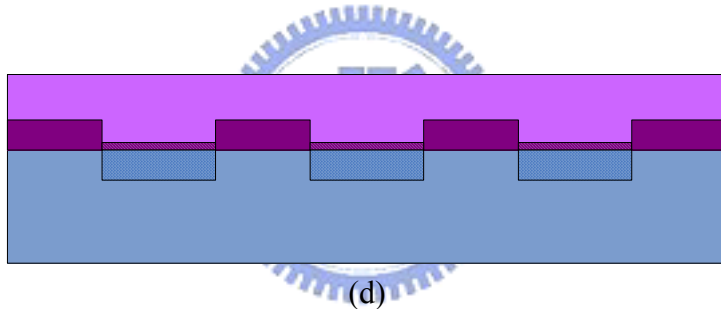
(d)
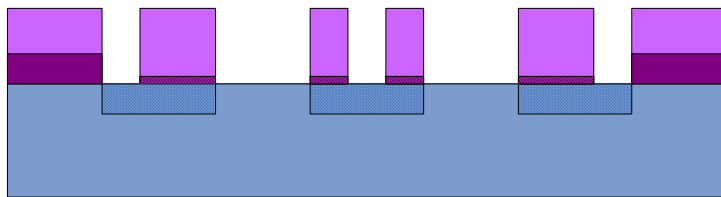
(e)
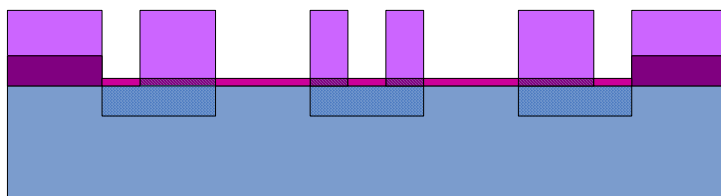
(f)
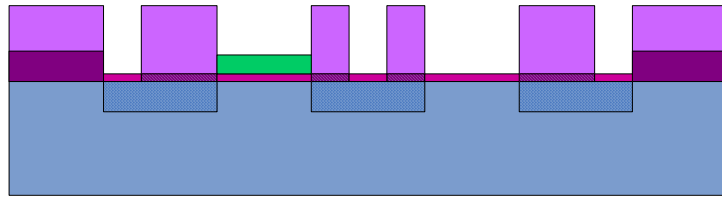
(g)
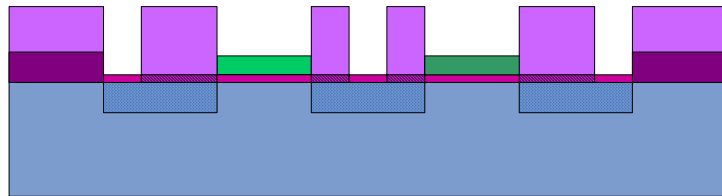
(h)
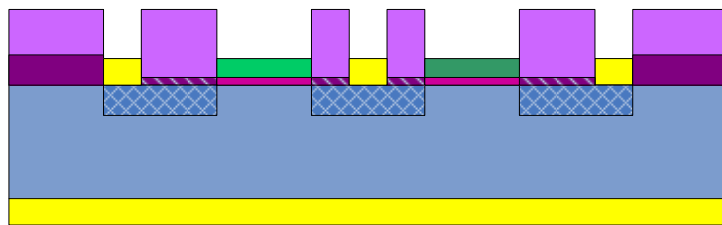
(i)

Fig. 3-1 Fabrication process flow
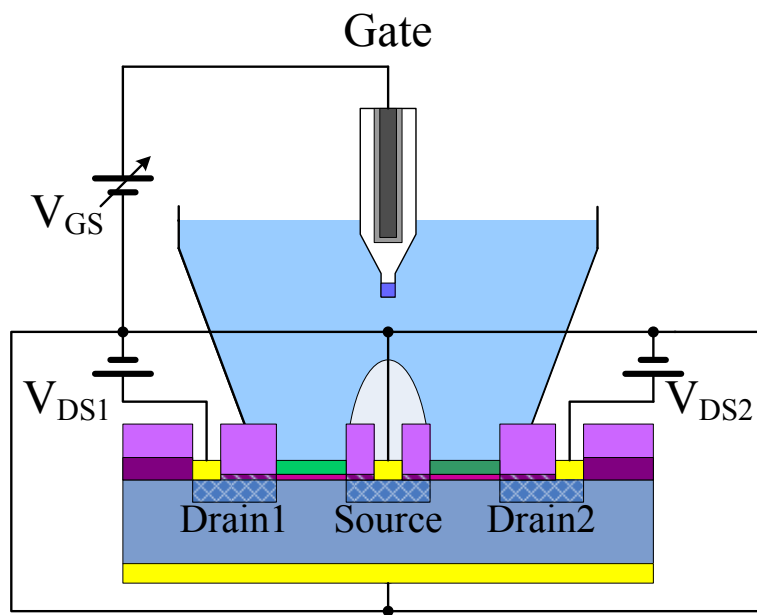
Fig. 3-2 Measurement setup
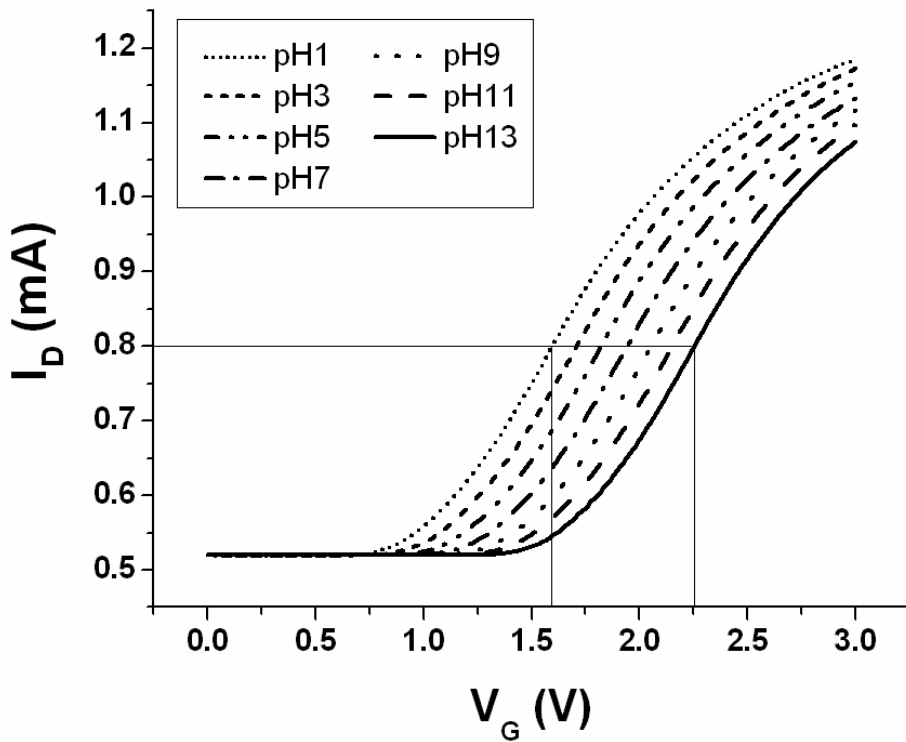
Fig. 3-3 Detection principle of pH
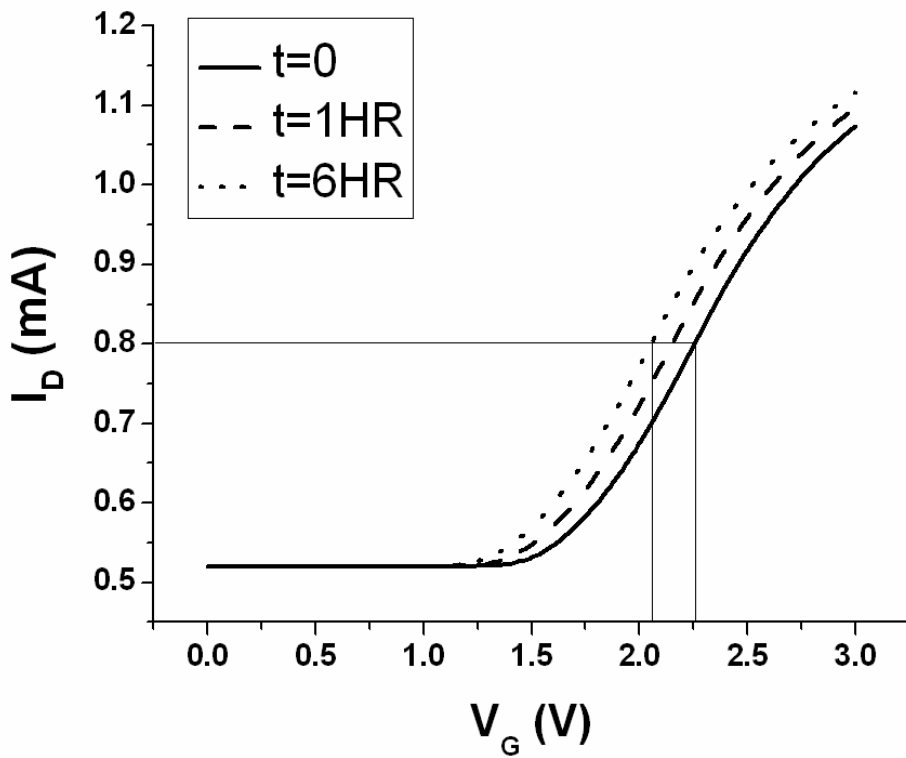
Fig. 3-4 Detection principle of drift
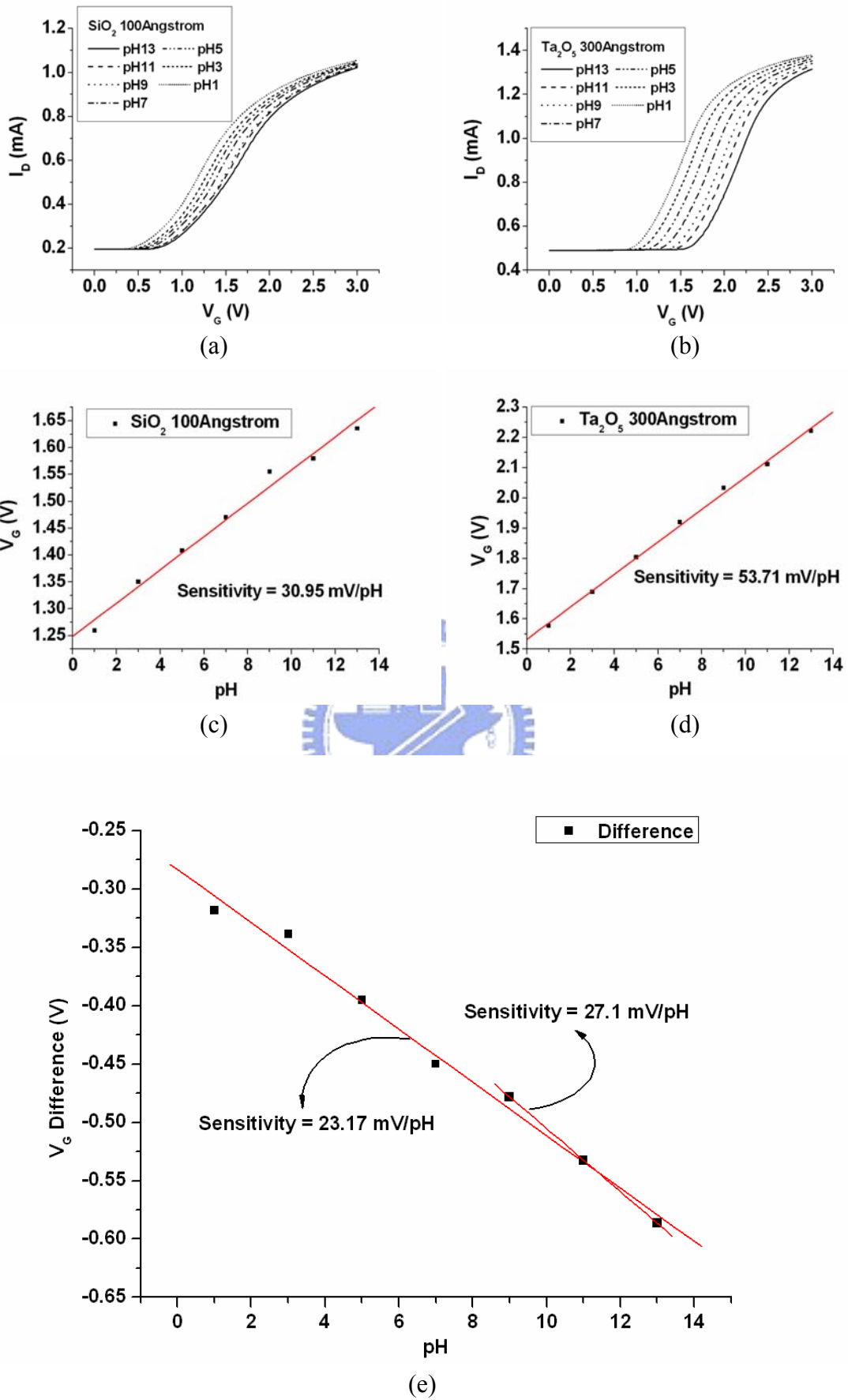
Fig. 4-1 Sensitivities of ISFET and REFET with x_U=100Å, W/L=400μm/20μm.
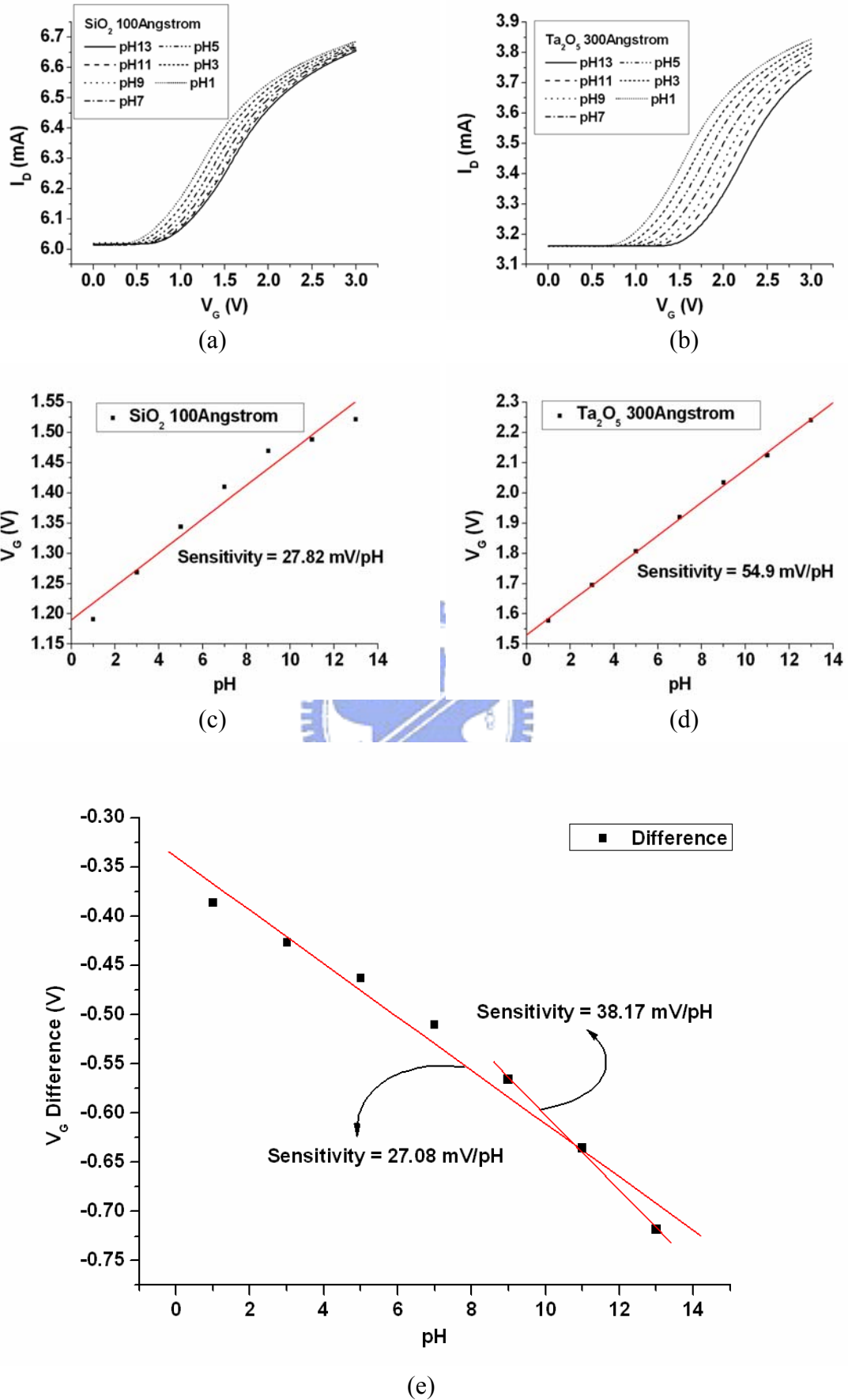
Fig. 4-2 Sensitivities of ISFET and REFET with x_U=100Å, W/L=400μm/30μm.
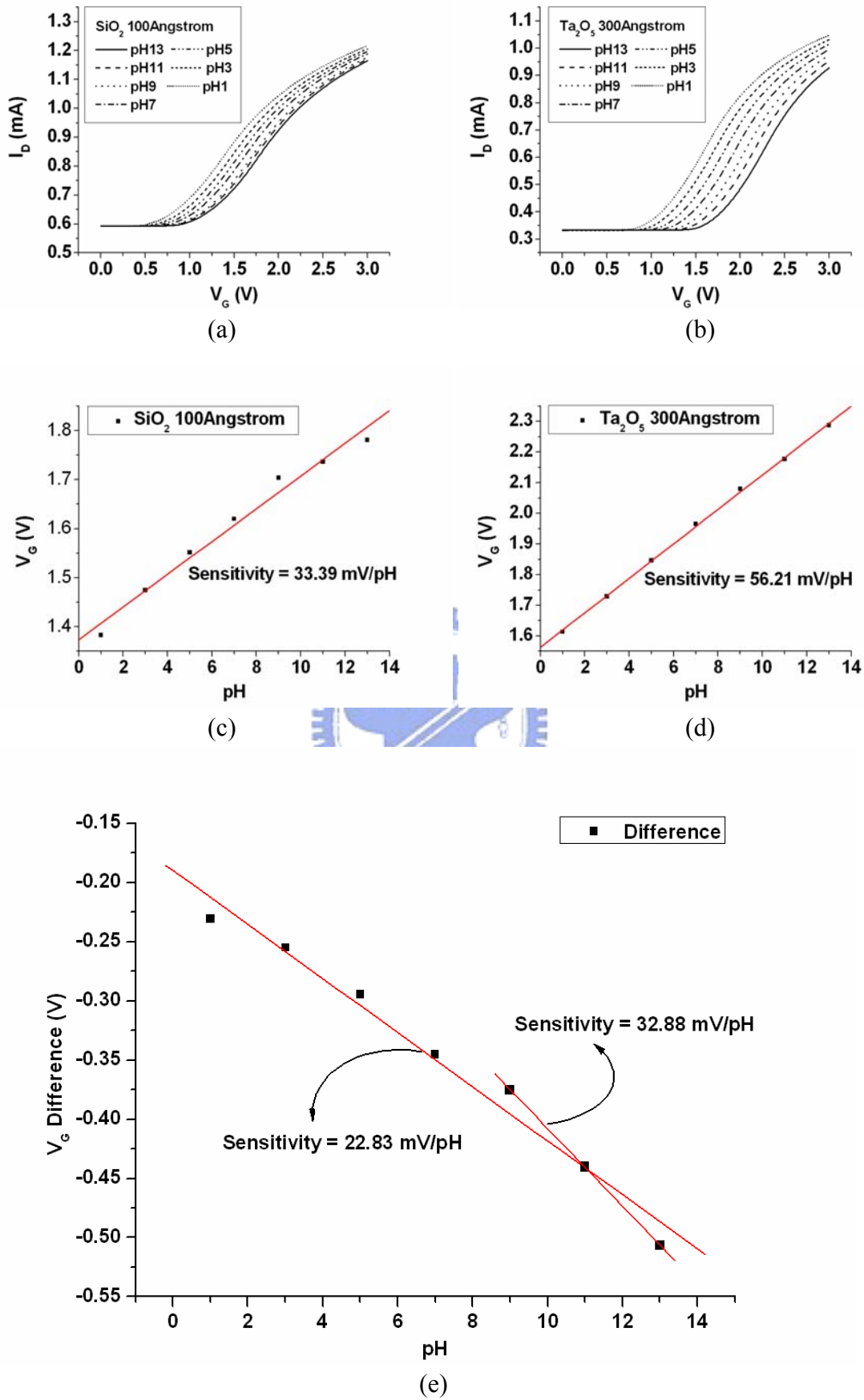
Fig. 4-3 Sensitivities of ISFET and REFET with x_U=100Å, W/L=400μm/40μm.
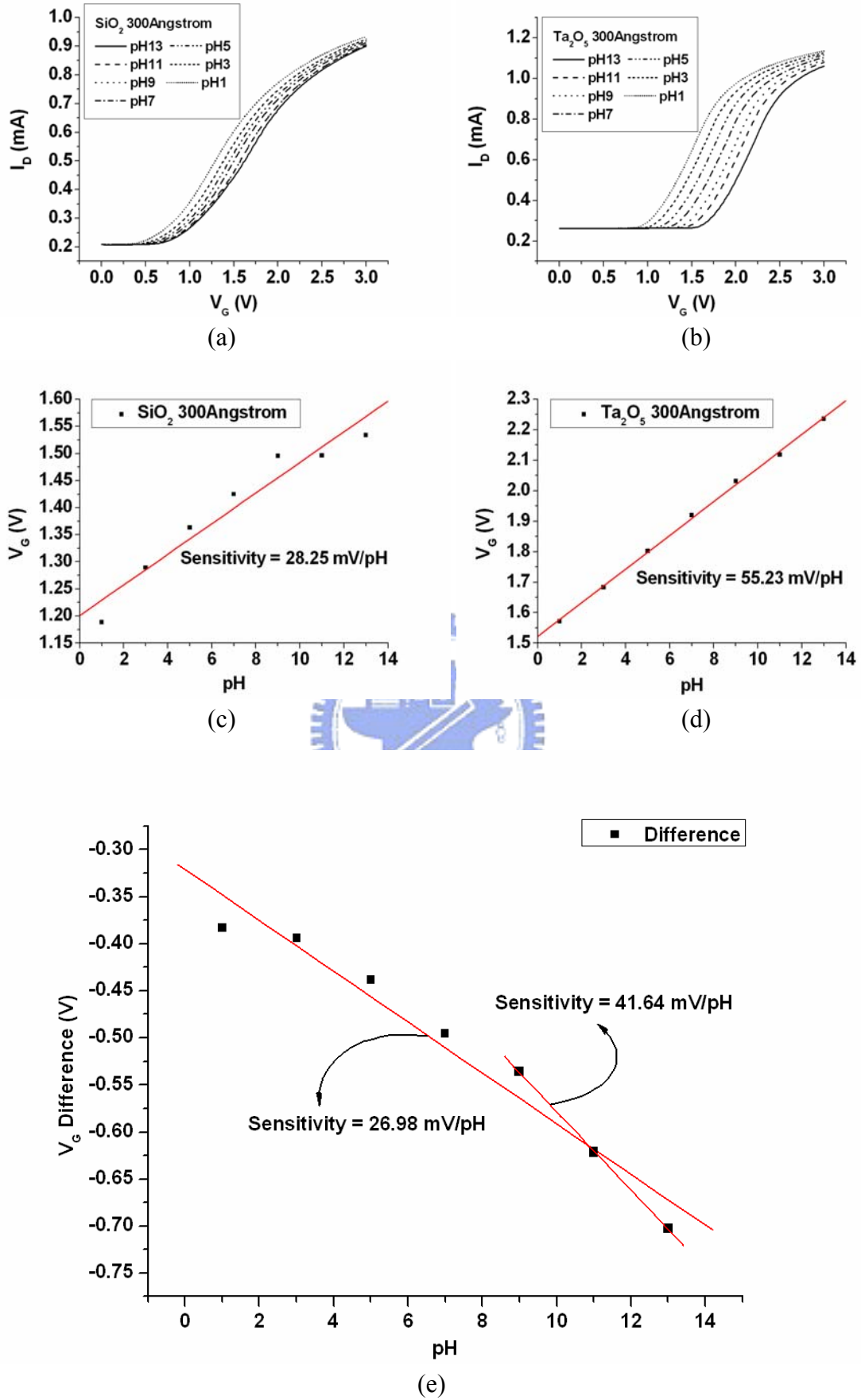
Fig. 4-4 Sensitivities of ISFET and REFET with x_U=300Å, W/L=400μm/20μm.

(a)

(b)

(c)

(d)

(e)
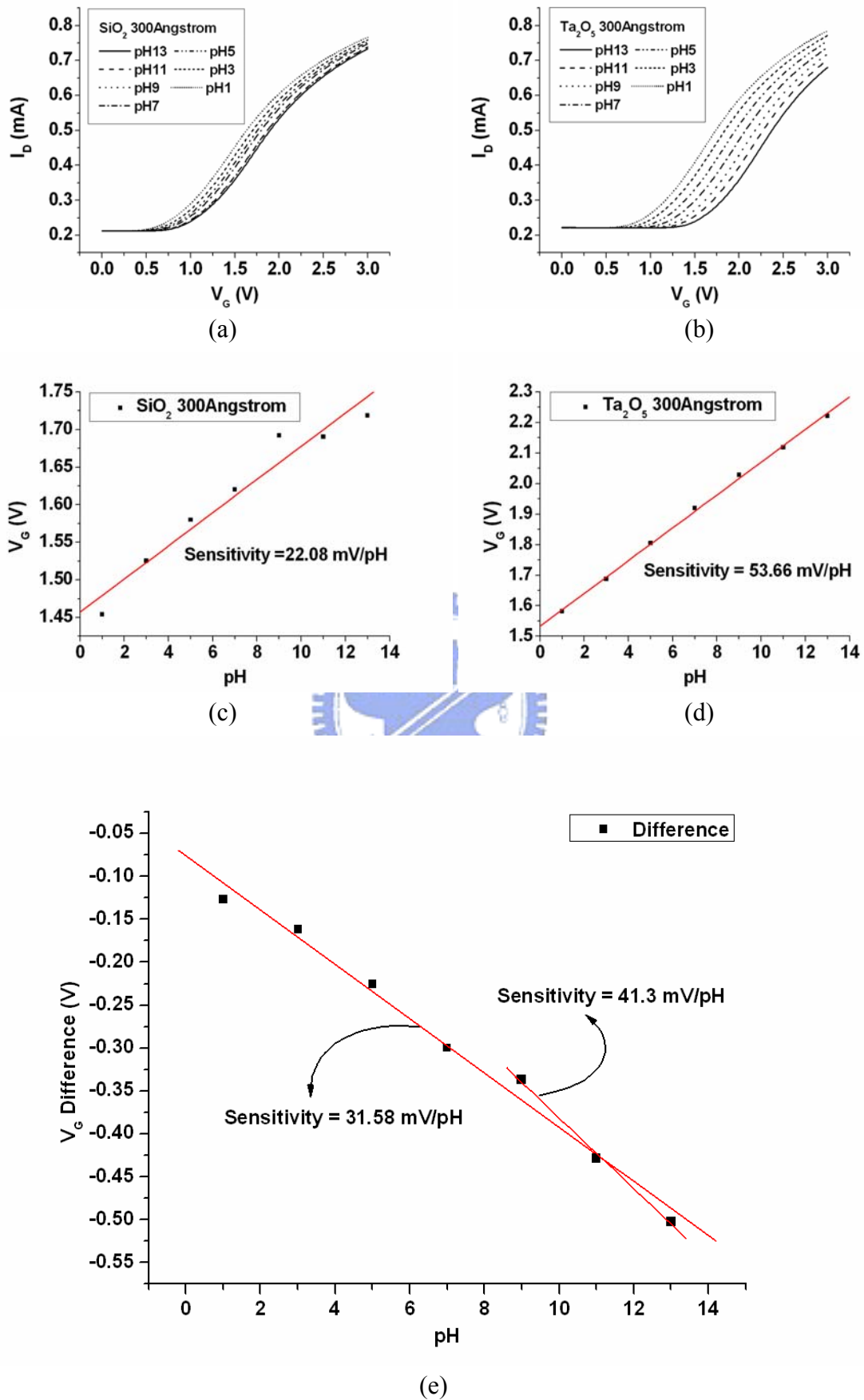
Fig. 4-5 Sensitivities of ISFET and REFET with x_U=300Å, W/L=400μm/30μm.
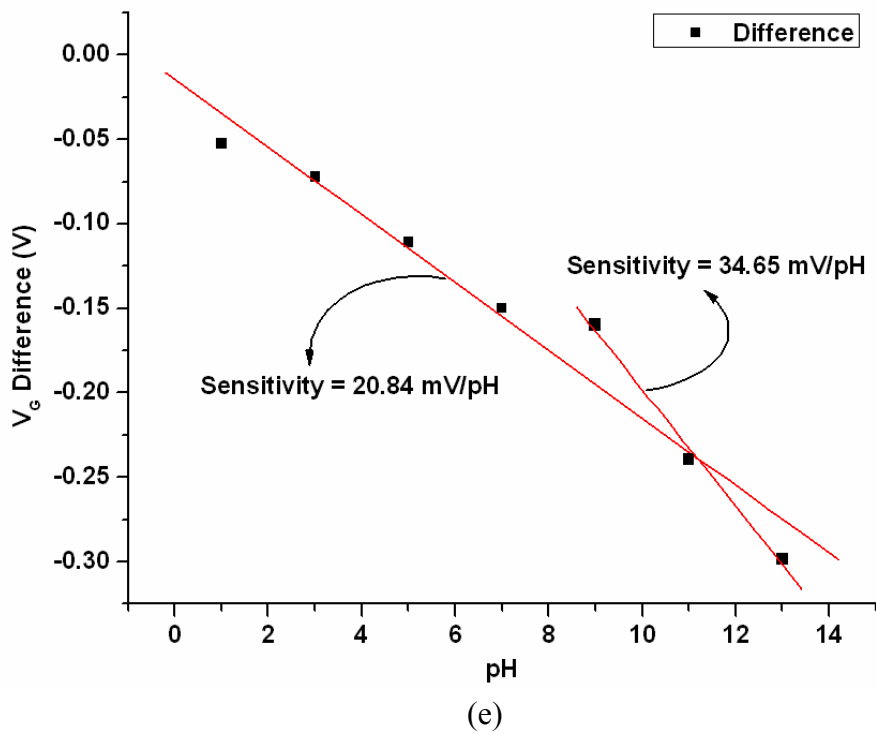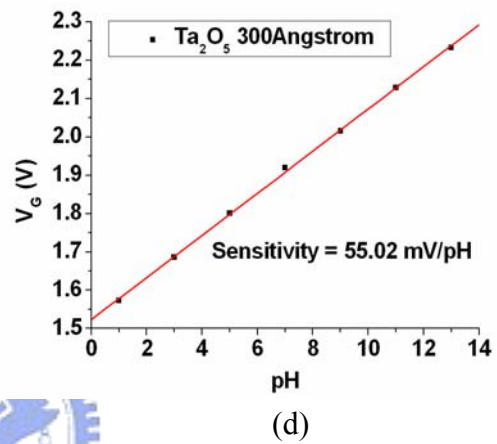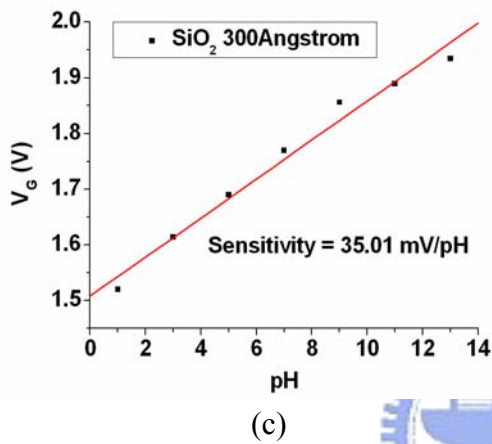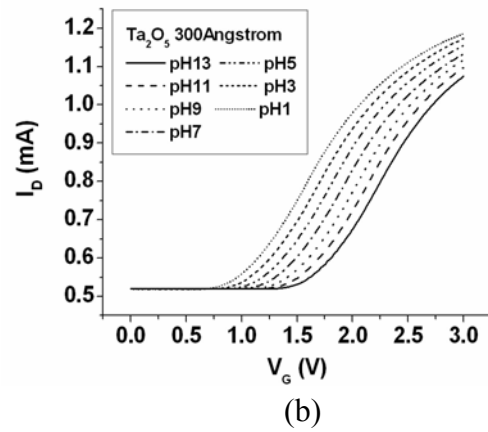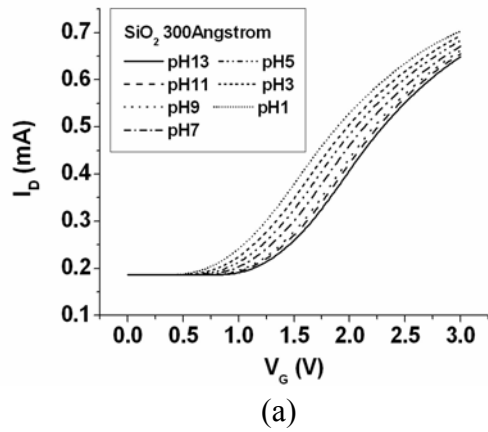
Fig. 4-6 Sensitivities of ISFET and REFET with x_U=300Å, *W/L*=400μm/40μm.
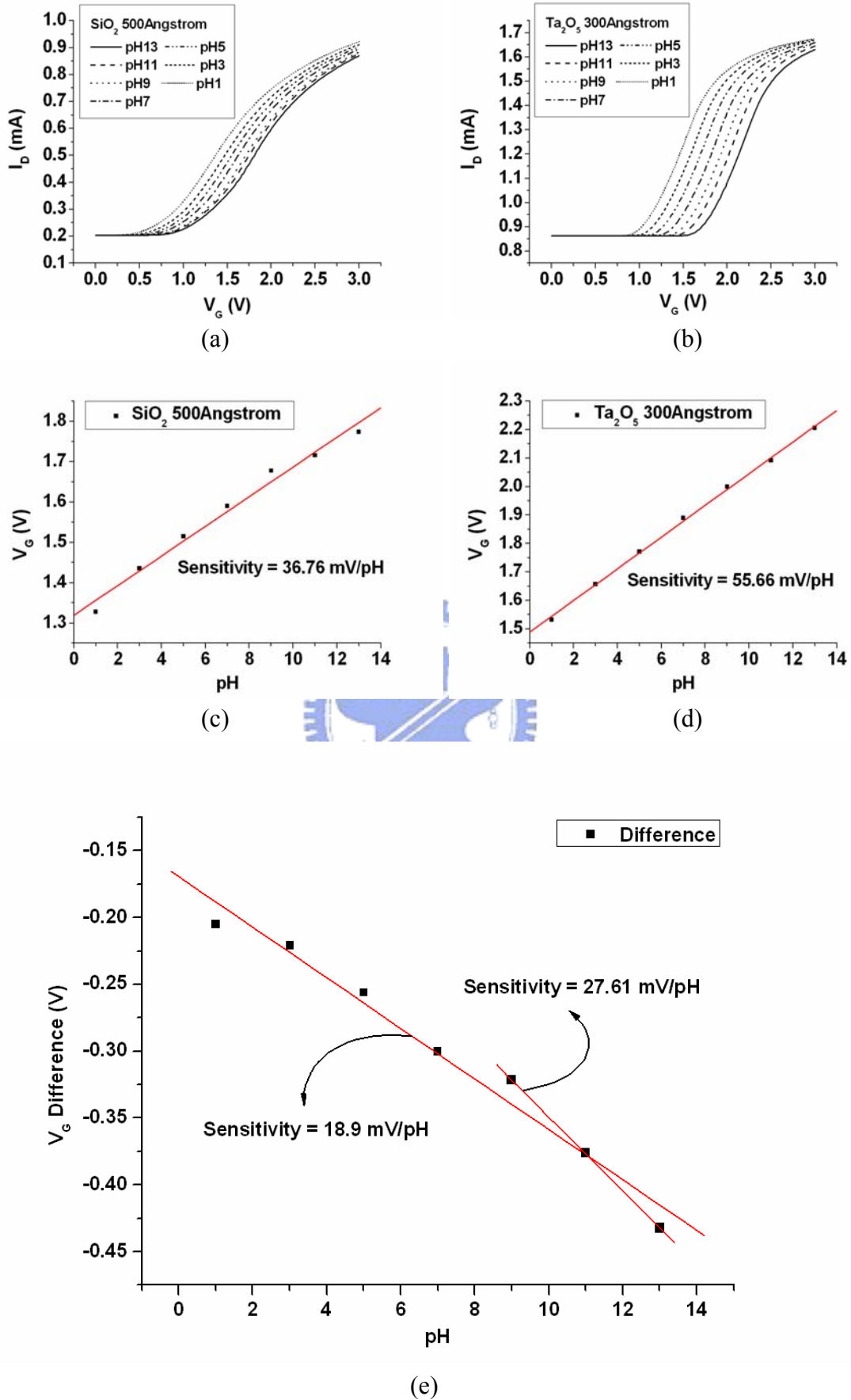
Fig. 4-7 Sensitivities of ISFET and REFET with x_U=500Å, W/L=400μm/20μm.
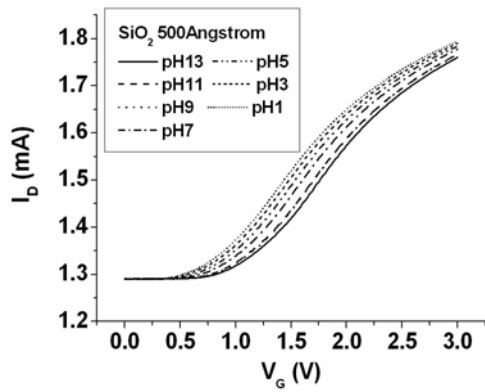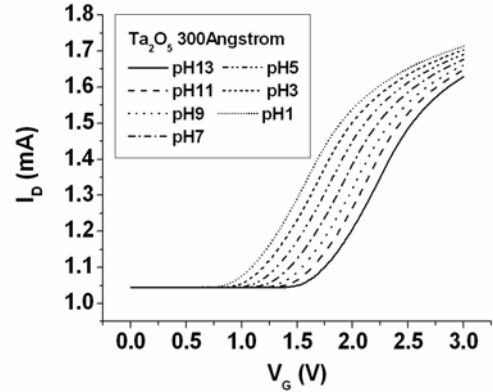
(a)   (b)
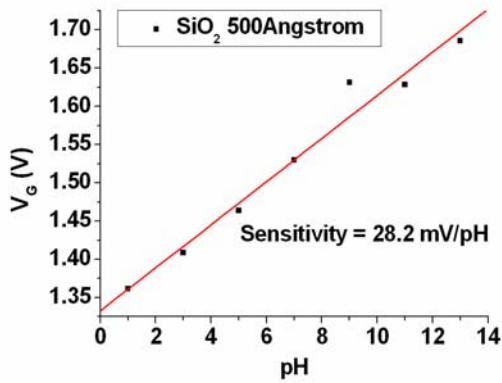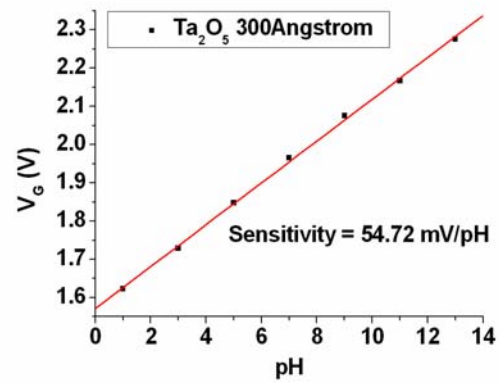
(c)   (d)
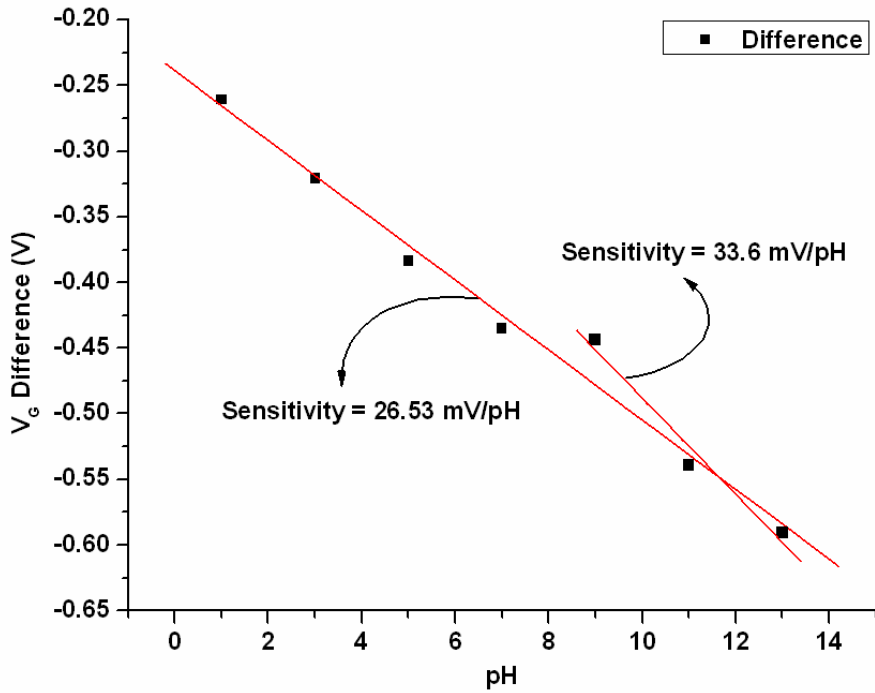
(e)

Fig. 4-8 Sensitivities of ISFET and REFET with x_U=500Å, W/L=400μm/30μm.
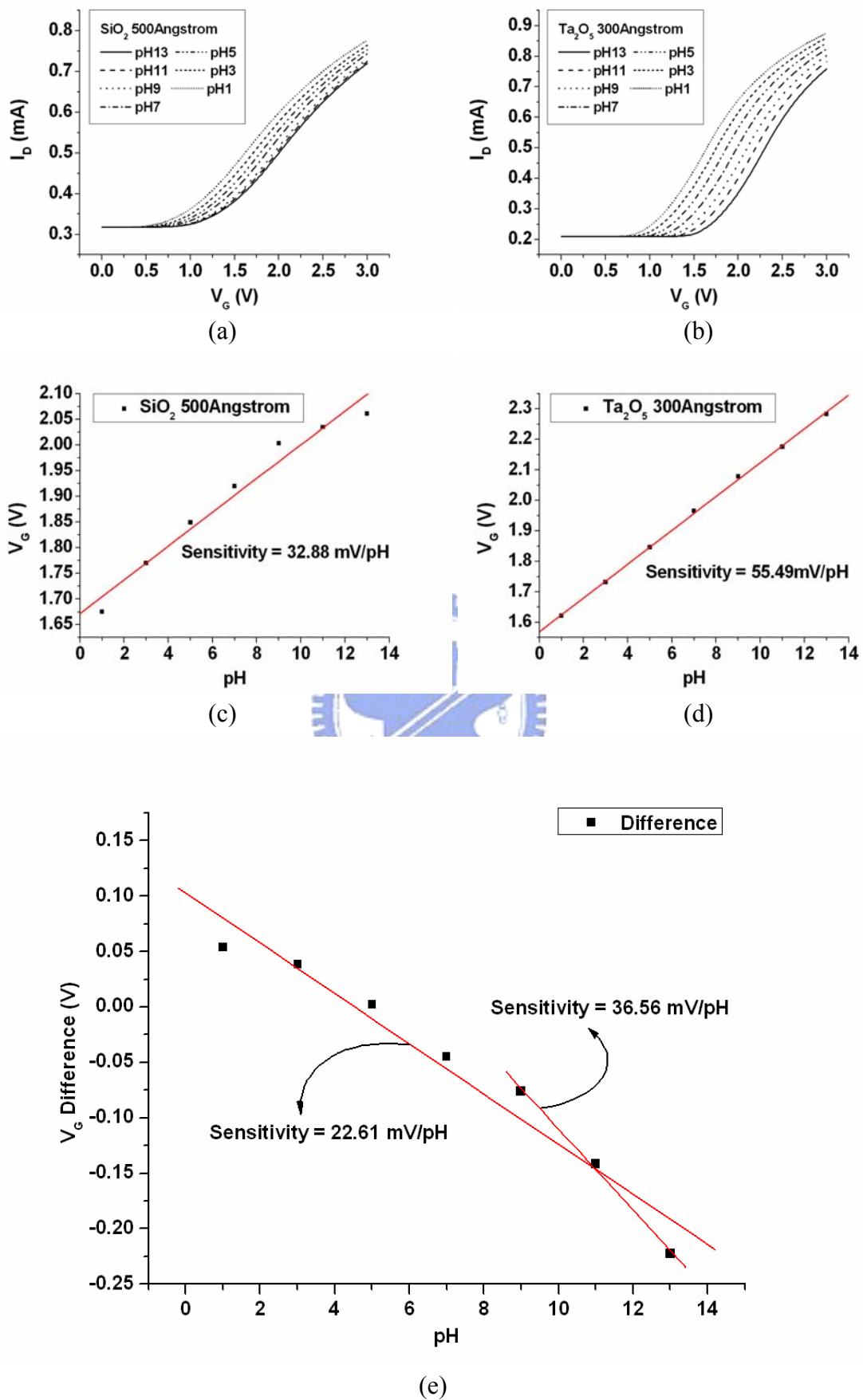
Fig. 4-9 Sensitivities of ISFET and REFET with x_U=500Å, *W/L*=400μm/40μm.
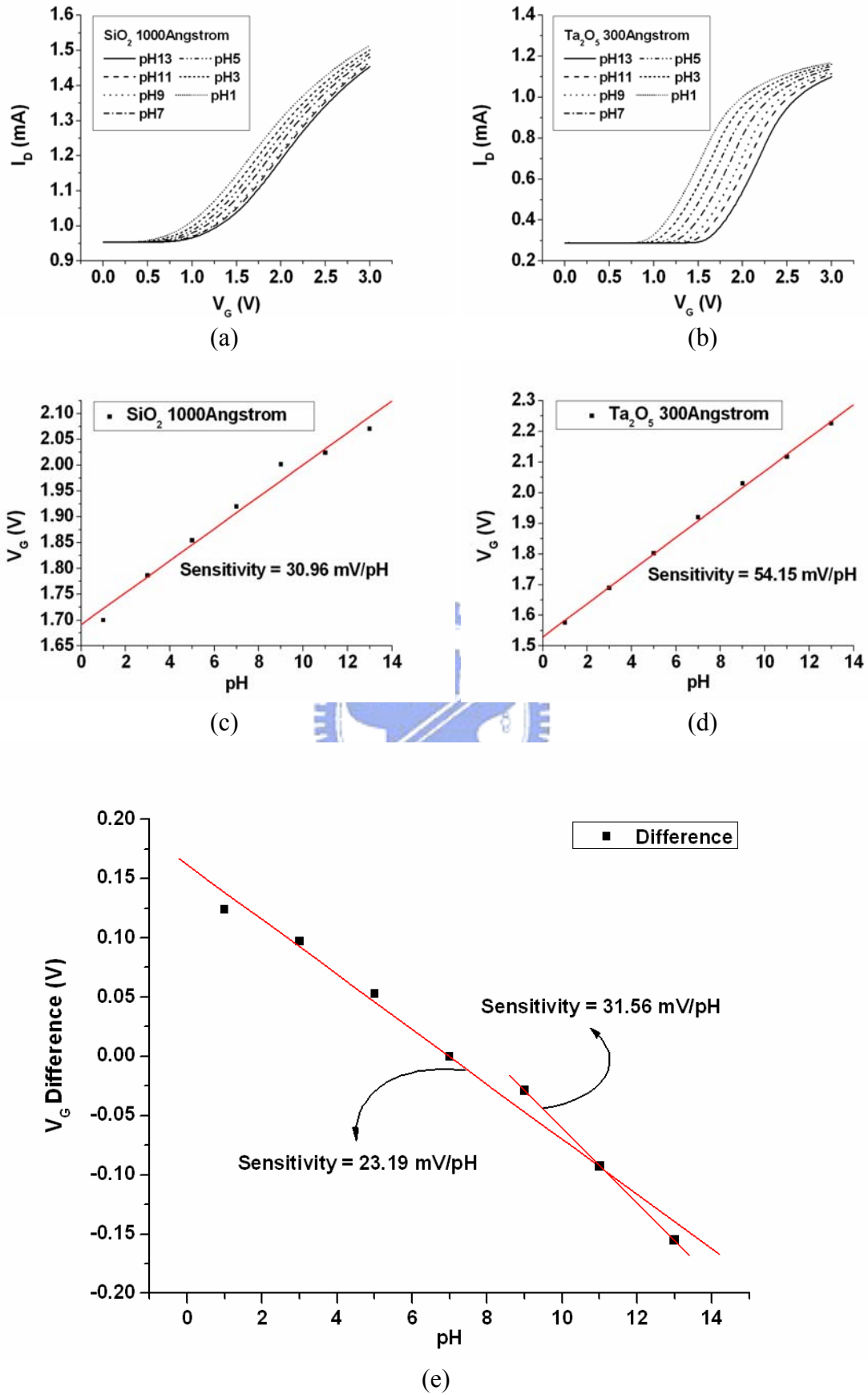
Fig. 4-10 Sensitivities of ISFET and REFET with x_U=1000Å, W/L=400μm/20μm.
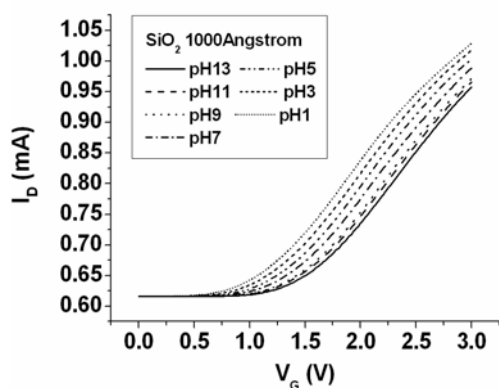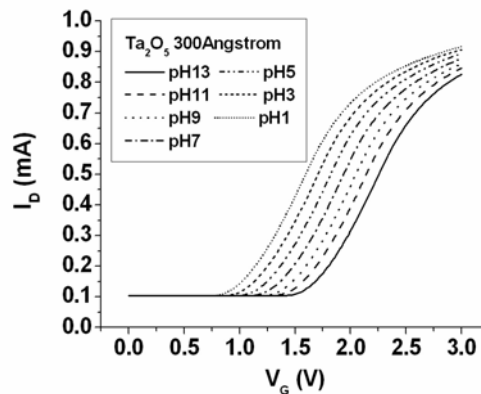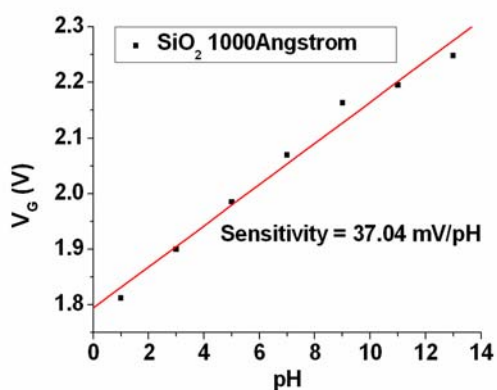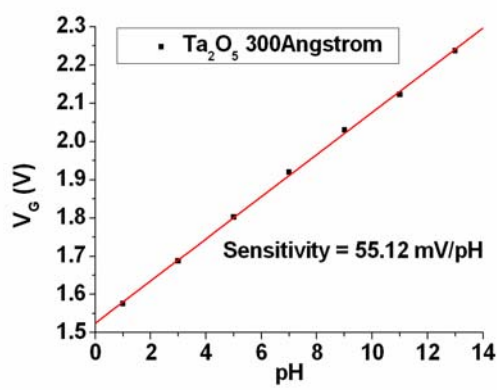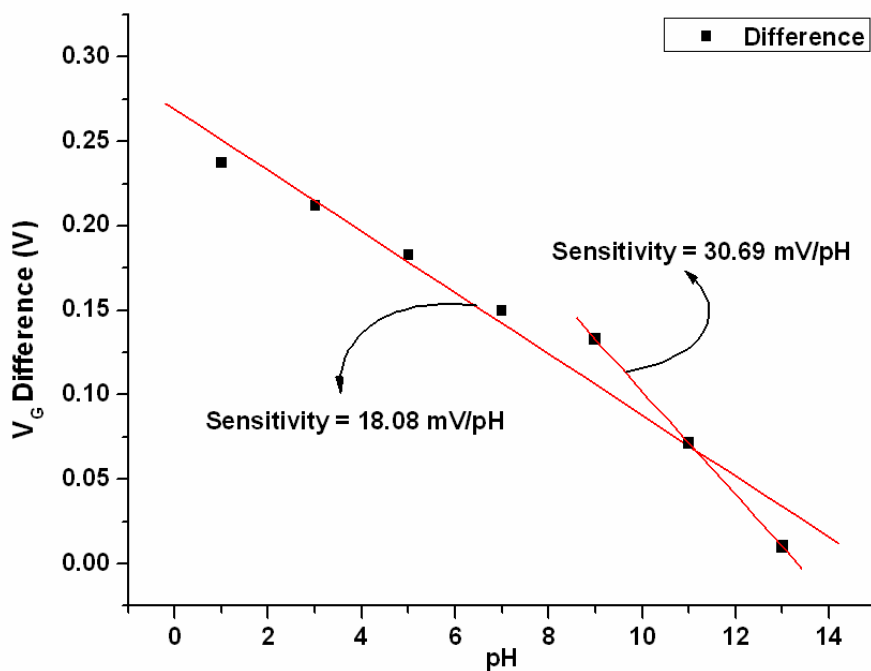
Fig. 4-11 Sensitivities of ISFET and REFET with x_U=1000Å, W/L=400μm/30μm.
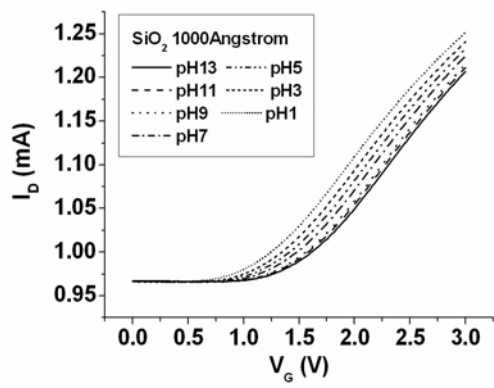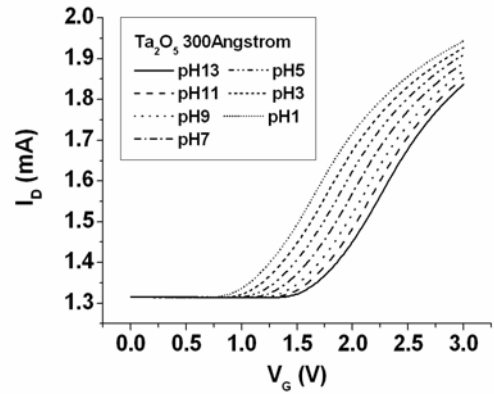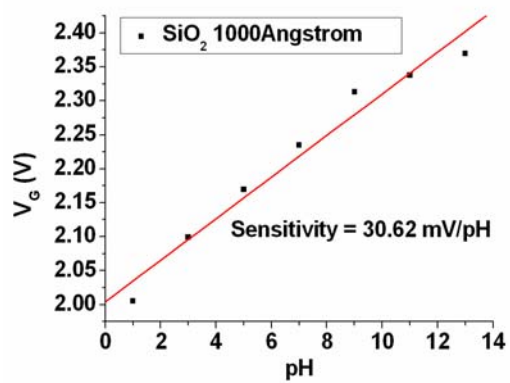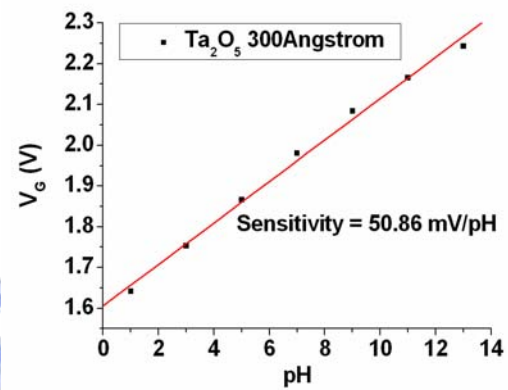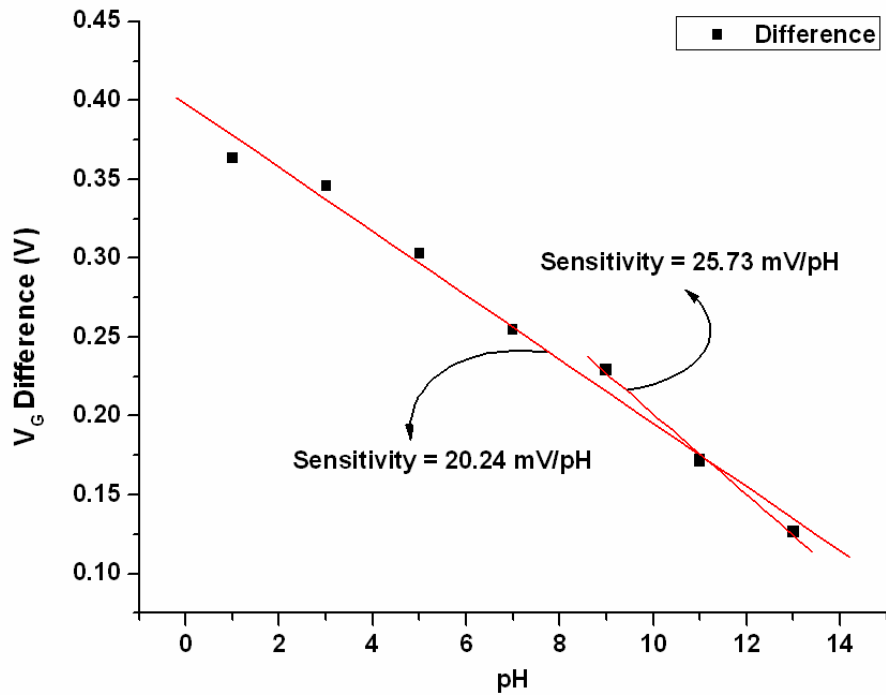
Fig. 4-12 Sensitivities of ISFET and REFET with x_U=1000Å, W/L=400μm/40μm.

	Sensitivity pH 1-13 (SiO_2 / Ta_2O_5)	Sensitivity pH 1-13 ($\triangle V_G$)	Sensitivity pH 1-9 ($\triangle V_G$)	Sensitivity pH 9-13 ($\triangle V_G$)
SiO_2 (100Å) W/L = 400/20	30.95 / 53.71	23.17	21.53	27.1
SiO_2 (100Å) W/L = 400/30	27.82 / 54.9	27.08	22.11	38.17
SiO_2 (100Å) W/L = 400/40	33.39 / 56.21	22.83	18.92	32.88
SiO_2 (300Å) W/L = 400/20	28.25 / 55.23	26.98	20.35	41.64
SiO_2 (300Å) W/L = 400/30	22.08 / 53.66	31.58	27.87	41.3
SiO_2 (300Å) W/L = 400/40	35.01 / 55.02	20.02	14.6	34.65
SiO_2 (500Å) W/L = 400/20	36.76 / 55.66	18.9	15.65	27.61
SiO_2 (500Å) W/L = 400/30	28.2 / 54.72	26.53	24.01	36.67
SiO_2 (500Å) W/L = 400/40	32.88 / 55.49	22.61	17.17	36.56
SiO_2 (1000Å) W/L = 400/20	30.96 / 54.15	23.19	20.15	31.56
SiO_2 (1000Å) W/L = 400/30	37.04 / 55.12	18.08	13.55	30.69
SiO_2 (1000Å) W/L = 400/40	30.62 / 50.86	20.24	17.97	25.73

Table 4-1 SiO_2 and Ta_2O_5 responses to pH electrolyte. $\triangle V_G$ is the difference between ISFET and REFET gate voltages.
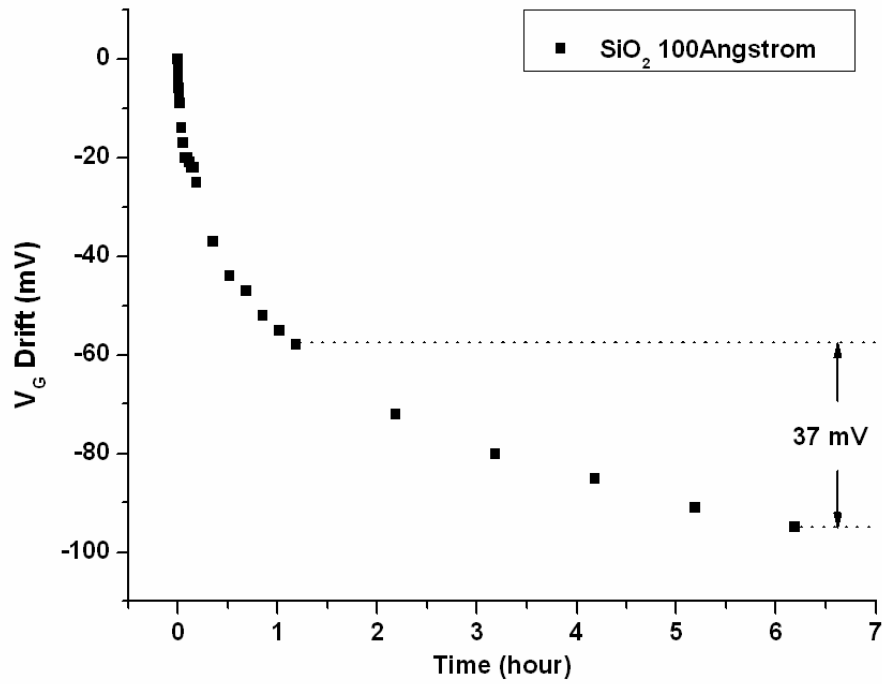
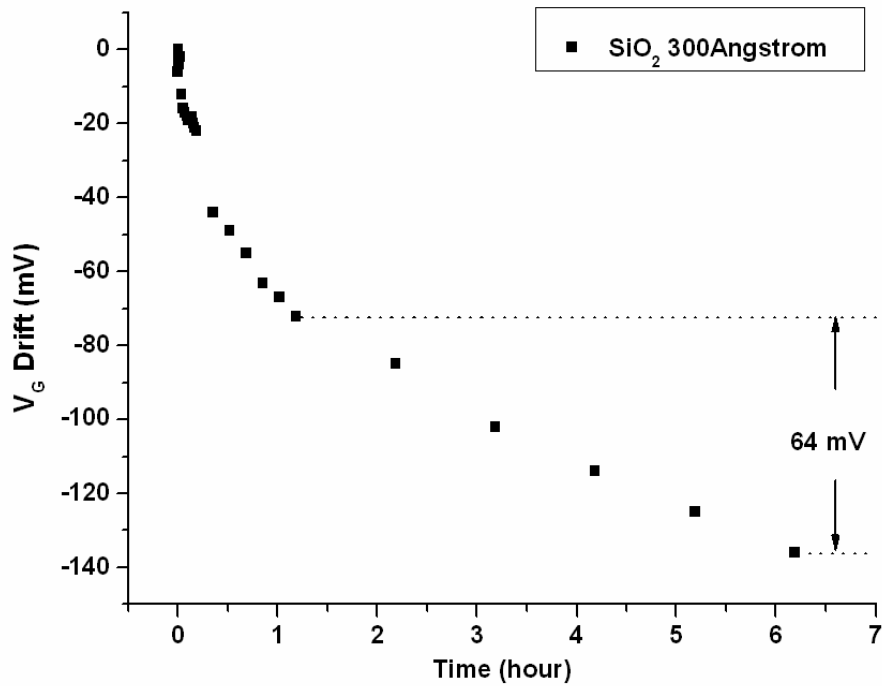Fig. 4-13 Drift characteristics of the 100Å PECVD SiO$_2$-gate ISFET.

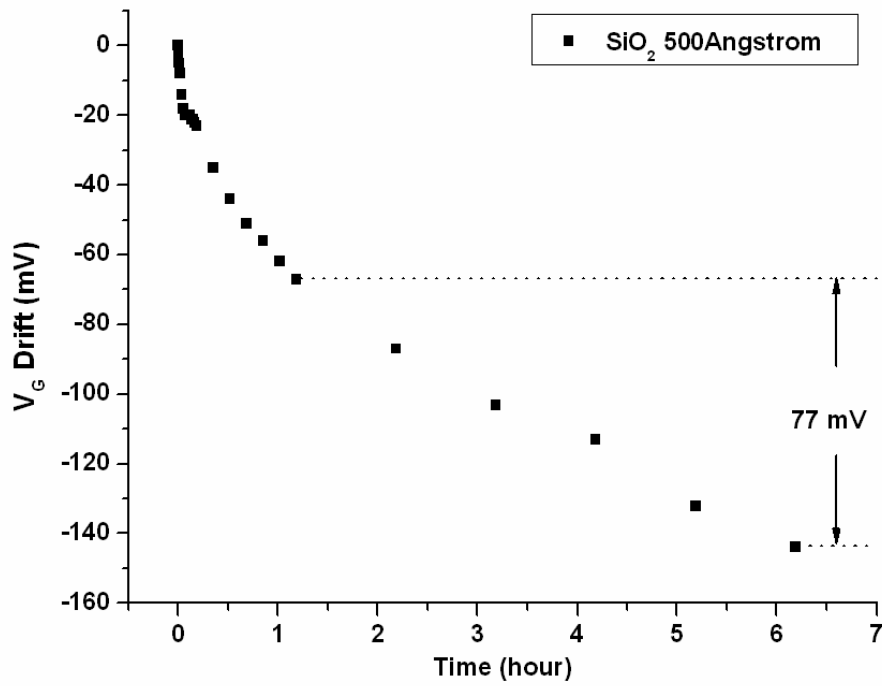Fig. 4-14 Drift characteristics of the 300Å PECVD SiO$_2$-gate ISFET.

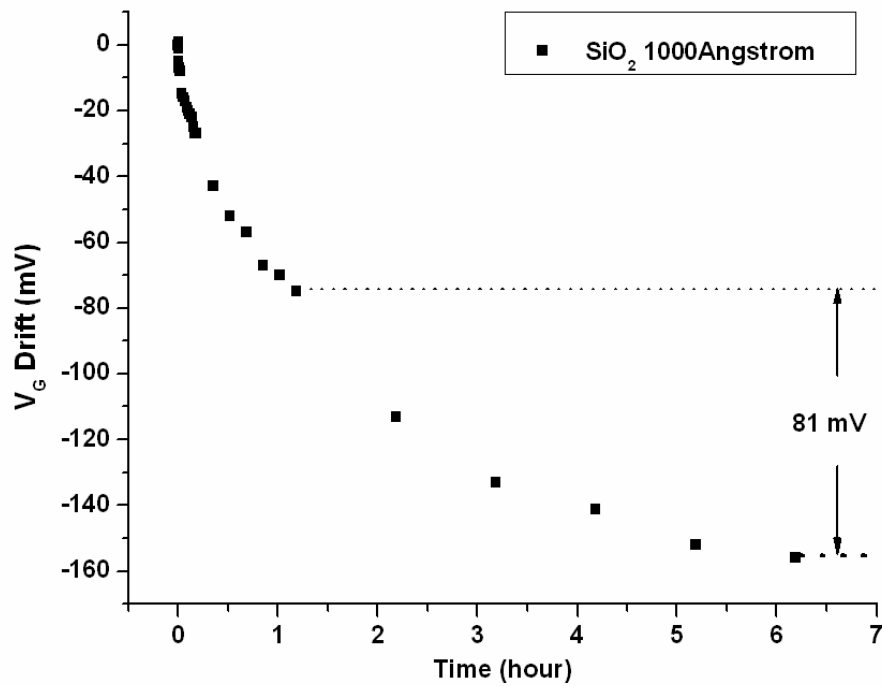Fig. 4-15 Drift characteristics of the 500Å PECVD SiO$_2$-gate ISFET.

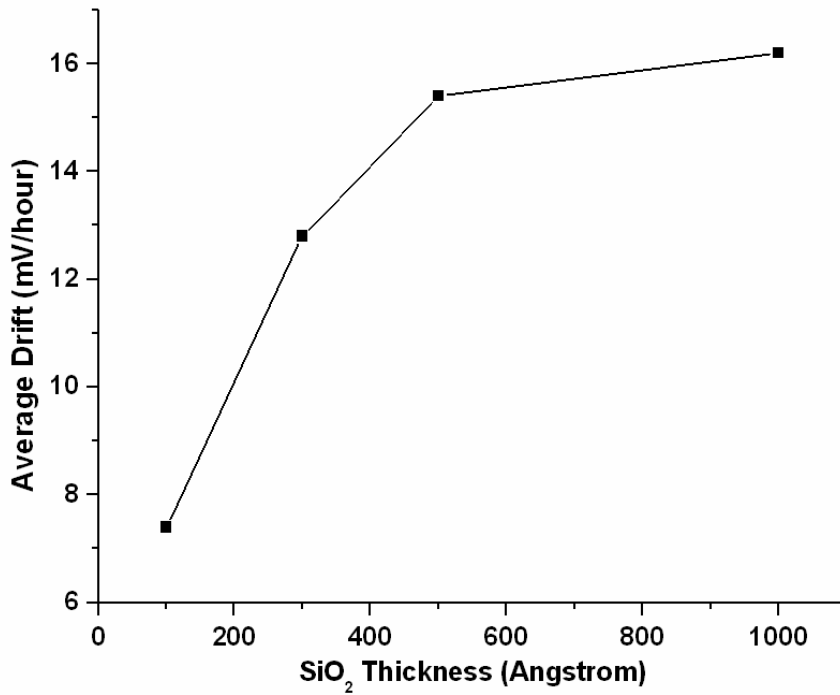Fig. 4-16 Drift characteristics of the 1000Å PECVD SiO$_2$-gate ISFET.

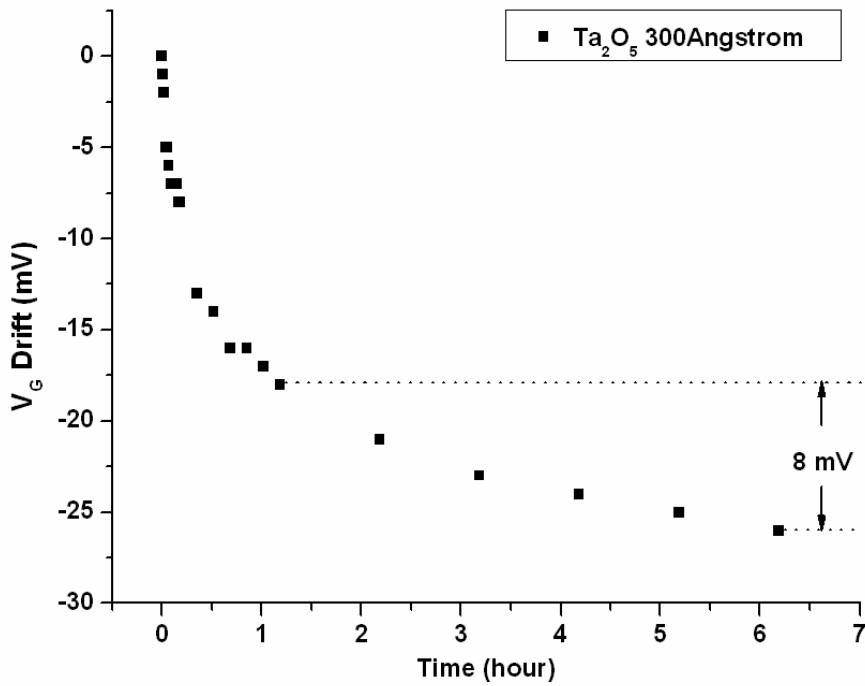Fig. 4-17 Average drift of the PECVD SiO$_2$-gate ISFET during the last 5 hour.

Fig. 4-18 Drift characteristics of the 300Å Ta$_2$O$_5$-gate ISFET.

	100Å PECVD SiO$_2$	300Å PECVD SiO$_2$	500Å PECVD SiO$_2$	1000Å PECVD SiO$_2$	300Å Sputtered Ta$_2$O$_5$
Average Gate-Voltage Drift (mV/hour)	7.4	12.8	15.4	16.2	1.6

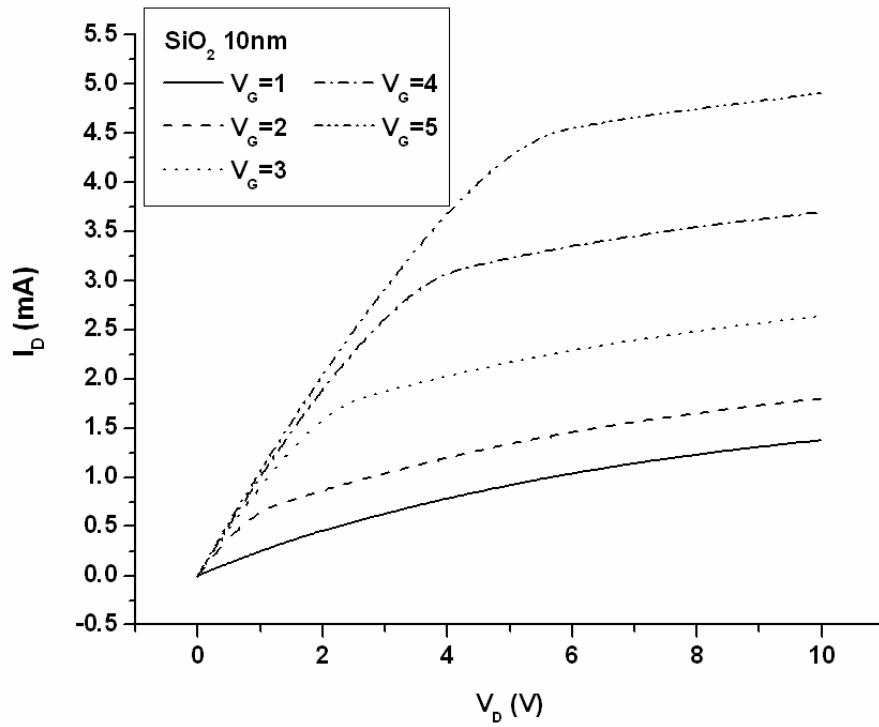Table 4-2 Average gate-voltage drift during the last 5 hour.

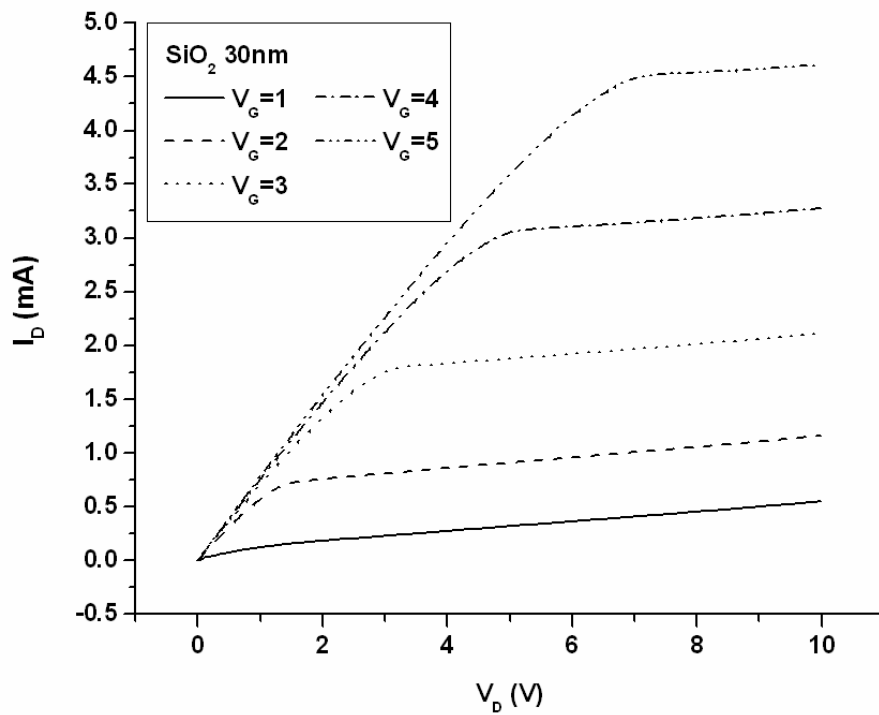Fig. 4-19 I_D-V_G curve of the 100Å SiO_2-gate ISFET.

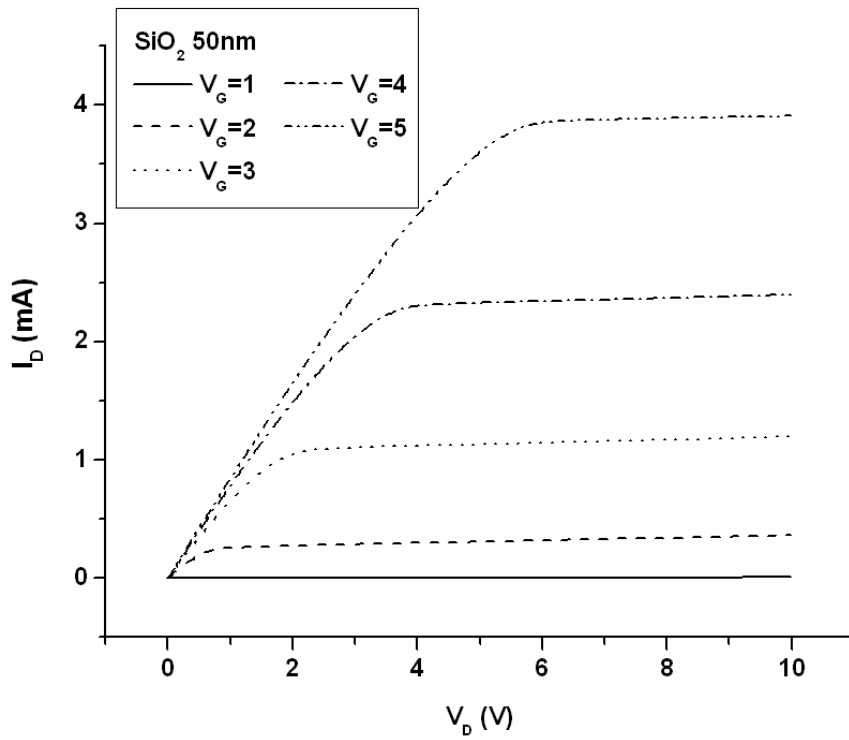Fig. 4-20 I_D-V_G curve of the 300Å SiO_2-gate ISFET.

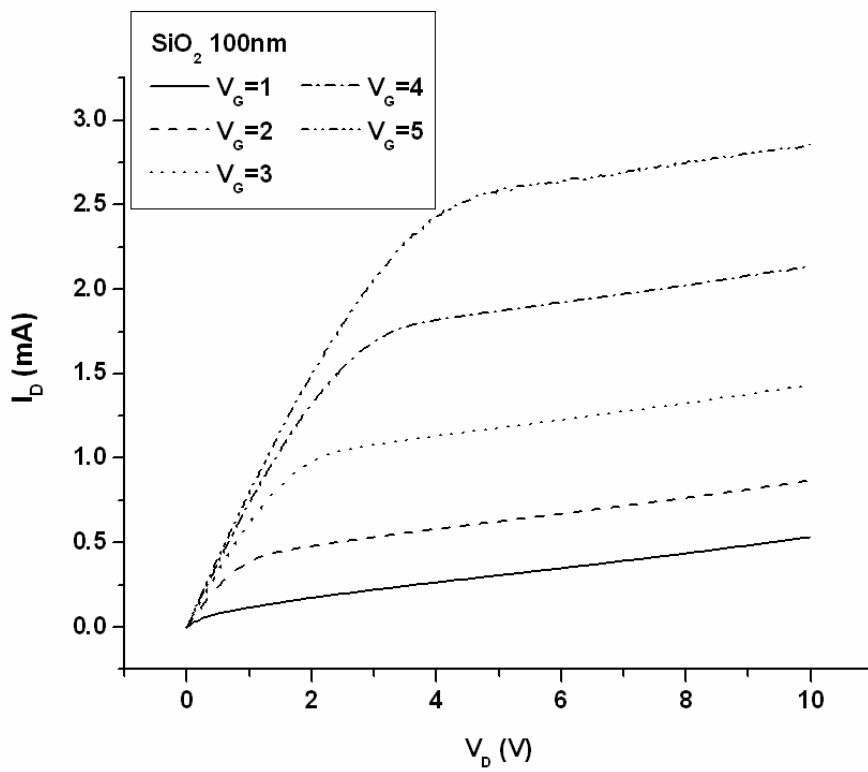Fig. 4-21 I_D-V_G curve of the 500Å SiO_2-gate ISFET.

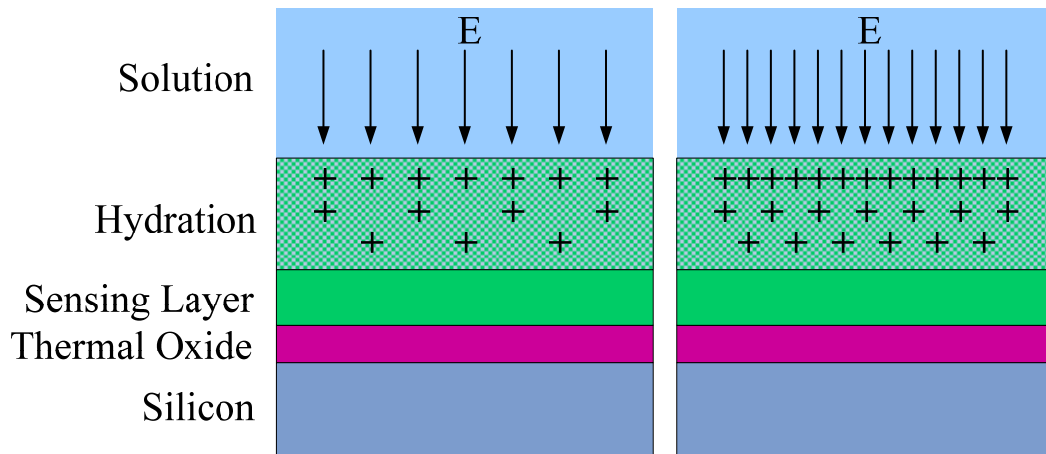Fig. 4-22 I_D-V_G curve of the 1000Å SiO_2-gate ISFET.

Fig. 5-1 The H$^+$ ions contamination influenced by the electric field strength.